Supporting Information to: Polychlorinated Biphenyls in a Temperate Alpine Glacier: 2. Model Results of Chemical Fate Processes

Christine Steinlin[1], Christian Bogdal[*,1,2], Pavlina A. Pavlova[3,4,5,6], Margit Schwikowski[4,5,6], Martin P. Lüthi[7,8], Martin Scheringer[1,9], Peter Schmid[3], and Konrad Hungerbühler[1]

[1] *Institute for Chemical and Bioengineering, Swiss Federal Institute of Technology, ETH Zurich, CH-8093 Zurich, Switzerland;*
[2] *Agroscope, Institute for Sustainability Sciences ISS, CH-8046 Zurich, Switzerland;*
[3] *Swiss Federal Laboratories for Materials Science and Technology (Empa), CH–8600 Dübendorf, Switzerland;*
[4] *Paul Scherrer Institute (PSI), CH–5232 Villigen, Switzerland;*
[5] *Oeschger Centre for Climate Change Research, University of Berne, CH–3012 Berne, Switzerland;*
[6] *Department of Chemistry and Biochemistry, University of Berne, CH–3012 Berne, Switzerland;*
[7] *Department of Geography, University of Zurich, CH–8057 Zurich, Switzerland;*
[8] *Laboratory of Hydraulics, Hydrology and Glaciology, Swiss Federal Institute of Technology, ETH Zurich, CH–8093 Zurich, Switzerland;*
[9] *Environmental Chemistry and Substance Dynamics, Leuphana University Lüneburg, 21335 Lüneburg, Germany*

Contents

List of Figures

List of Tables

S1 Chemical Fate Modeling

The model is a dynamic multimedia chemical fate model, describing the fate of a chemical in a specific system. For this, the system is divided into well-mixed compartments each one having specific properties. All processes, such as losses from the system or inter-compartmental transfer are described by first-order differential equations. The processes are variable in time and specific for each compartment. A differential equation describing the amount of chemical in a compartment is set up for every compartment (Equation (S1)), where N is the amount of chemical in the compartment (mol), I is the inflow into the compartment from outside the system (mol month^{-1}), D is the sum of all loss and transfer processes from and to the other compartments as well as leaving the system (mol Pa^{-1} h^{-1}), V is the volume of the compartments (m^3), and Z is the fugacity capacity of the compartments (mol Pa^{-1} m^{-3}). While N, I, V, and Z are vectors with a length equal to the number of compartments, D is a matrix with a size equal to the number of compartments in two dimensions. N, I, V, Z, and D change with time, in this model in a monthly resolution from January 1900 to December 2010.

$$\frac{dN}{dt} = I + D * \frac{N}{V * Z} \tag{S1}$$

The model is fugacity-based, where concentration (C, mol m^{-3}), fugacity (f, Pa), and fugacity capacity (Z, mol Pa^{-1} m^{-3}) are connected by Equation (S2).

$$C = Z * f \tag{S2}$$

D-values of advection (D_{adv}) are calculated from the amount of medium advected out of the system during a period of time (G, m^3 month^{-1}), D-values of degradation (D_{deg}) are calculated from rate constants (k, month^{-1}) and the volume (V, m^3), and D-values of mass transfer (D_{mtr}) are calculated from mass transfer coefficients (k_{m}, m^3 m^{-2} month^{-1}) and the area (A, m^2) (Equations (S3)–(S5)).

$$D_{\mathrm{adv}} = G * Z \tag{S3}$$
$$D_{\mathrm{deg}} = k * V * Z \tag{S4}$$
$$D_{\mathrm{mtr}} = k_{\mathrm{m}} * A * Z \tag{S5}$$

The fugacity concept was used numerous times before and described in detail in Mackay [24].

S2 Solving the System of Chemical Mass Balance Equations

The system of mass balance equations is solved numerically using the Matlab built-in solver ode15s. In order to track all fluxes (losses and transfers) in the system and to close the mass balance of the chemical for every time unit and compartment, we expand the system in Equation (S1) by adding a copy of every compartment to the system. If there are four compartments, the vectors I, V and Z in Equation (S1) are expanded from 4x1 to 8x1, while the D-matrix is expanded from 4x4 to 8x8. For the copied compartments, the input I is zero, and V and Z can be set to any number (e.g. the same as the original compartment) as no fluxes are leaving these compartments.

The upper left part of the D-matrix (4x4) stays the same (original D-matrix). In the diagonal of this part, the D-values of all processes leaving the compartments can be found, loss processes as well as transfer processes. These values are used as input to the copied compartments (as positive values). This means that now, the mass leaving a specific compartment is still transferred to the original destination (defined by the original part of the D-matrix), but at the same time, a copy of this mass is passed on to the copied compartments. In these compartments, the mass accumulates until we set it back to zero (e.g. at the end of the month or the time unit we are interested in). Here is an example for four compartments.

Original D-matrix:
$$\begin{bmatrix} -D & + & + & + \\ + & -D & + & + \\ + & + & -D & + \\ + & + & + & -D \end{bmatrix}$$

D-matrix including copied compartments:
$$\begin{bmatrix} -D & + & + & + & 0 & 0 & 0 & 0 \\ + & -D & + & + & 0 & 0 & 0 & 0 \\ + & + & -D & + & 0 & 0 & 0 & 0 \\ + & + & + & -D & 0 & 0 & 0 & 0 \\ +D & 0 & 0 & 0 & 0 & 0 & 0 & 0 \\ 0 & +D & 0 & 0 & 0 & 0 & 0 & 0 \\ 0 & 0 & +D & 0 & 0 & 0 & 0 & 0 \\ 0 & 0 & 0 & +D & 0 & 0 & 0 & 0 \end{bmatrix}$$

In addition to knowing the mass that has left a specific compartment, we also want to know which process is responsible for which amount of the transferred mass. For this, we can benefit from the additivity of the D-values (Equation (S6)), where F_i is the amount of chemical transferred by process i (mol month^{-1}), F_{tot} is the total amount of chemical leaving a specific compartment (mol month^{-1}), D_i is the D-value of process i (mol Pa^{-1} h^{-1}), and D_{tot} is the sum of the total D-values found in the diagonal of the original D-matrix (mol Pa^{-1} h^{-1}).

$$F_i = F_{\text{tot}} * \frac{D_i}{D_{\text{tot}}} \tag{S6}$$

This approach enables us to keep track of all fluxes in the system, losses and transfer fluxes from all compartments in all time units, and we can verify the model by closing the mass balance of the chemical in our system for every compartment and time unit.

S3 Study sites on the Silvretta glacier

Silvretta glacier and the three study sites are shown in Figure S1. The accumulation area is located in the eastern part of the glacier, the ablation area is located in the western part. The glacier flows from east to west.

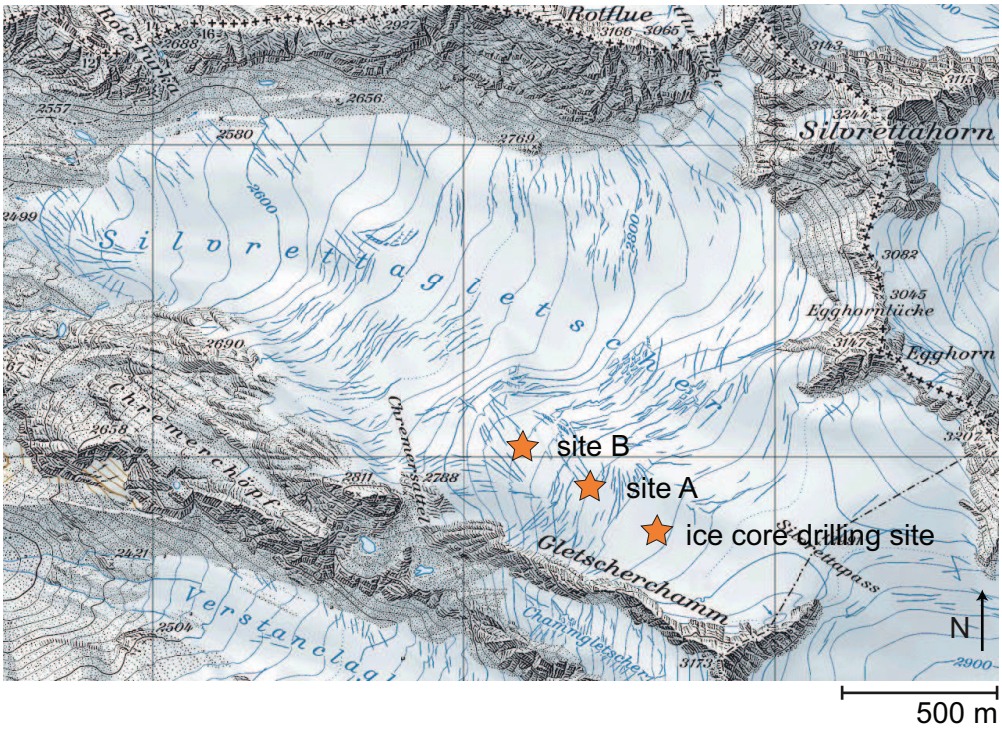

Figure S1: Silvretta glacier with the three sites (ice core drilling site, site A, and site B) indicated by orange stars. (©2014 swisstopo (JD100042))

S4 Environmental System

S4.1 Input Parameters

Air temperature on Silvretta glacier (2500–3000 m a.s.l., Figure S2) is calculated from measured monthly air temperatures from Weissfluhjoch (2700 m a.s.l., 1959–2010) and Säntis (2500 m a.s.l., 1900–1959), two meteorological stations in Eastern Switzerland. All stations are indicated on Figure S3. Air temperature is corrected for elevation differences using a temperature gradient of 0.83 °C/100 m. This gradient was calculated using a dry adiabatic gradient of 1 °C/100 m and a saturated adiabatic temperature gradient of 0.65 °C/100 m (valid in the middle troposphere) [43]. The average of these two gradients corresponds to the 0.83 °C/100 m used in the model, as the ratio of rain days in the Swiss Alps was 50% between 1961 and 2002 (days with precipitation higher than 0.1 mm, data for Kleine Scheidegg, a station close to Jungfraujoch) [40].

The first glacier snow accumulation (mass balance) measurements on Silvretta glacier were done in 1915, resulting in one of the longest mass balance measurement series existing [22, 21, 42]. Snow accumulation is measured by placing stakes on the glacier surface and determining the change in snow mass after a specific period of time. Spatially distributed winter and summer mass balances were determined by calibrating a mass balance model of Silvretta glacier with ice volume changes from high-resolution digital elevation models, point-based mass balance measurements and discharge records, using air temperature and precipitation data from two high-altitude meteorological stations [22, 21]. The resulting mass balance grid data was then combined for 71 glacier sections located perpendicular to the main flowline of the glacier. The local snow accumulation for the ice core site, site A, and site B is shown in Figure S4. While the winter balance is in the same range for all sections, the annual balance is higher on the ice core site, located at a higher elevation than sites A and B. After 1990, the annual mass balance decreases markedly.

Wind speed, precipitation, and the volume fraction of aerosol particles in the atmosphere are temporally resolved, but equal for all sites of the glacier. Monthly wind speed measurements from Weissfluhjoch are available from 1959 to 2010 [40]. Between 1900 and 1958, the wind speed of the period 1959–1987 is used. Monthly precipitation measurements from Weissfluhjoch (1959–2010) and Davos (1900–1958) are normalized to the average annual precipitation measured on the Silvretta glacier forefield [40]. Precipitation is set equal to the snow accumulation during winter. Precipitation occurs as rain during summer and as snow during winter. During winter, precipitation induces wet gaseous and particle deposition to the glacier surface. During summer, wet gaseous and particle deposition is described as a loss process from the system, assuming the rain to run off from the glacier before interacting with the glacier surface. Refreezing of rainwater in the glacier is neglected. Monthly measurements of particulate matter (PM10) from Jungfraujoch (1973–2010, 3600 m a.s.l., 130 km from Silvretta glacier) are used to describe the fraction of aerosol particles in the model [28]. These measurements are available between 1973 and 2010. Between 1900 and 1972, monthly resolved PM10 values are estimated from the monthly measurements between 1973 and 2010, normalized to black carbon emissions in early and late decades in the 20th century, as estimated by Bond et al. [6].

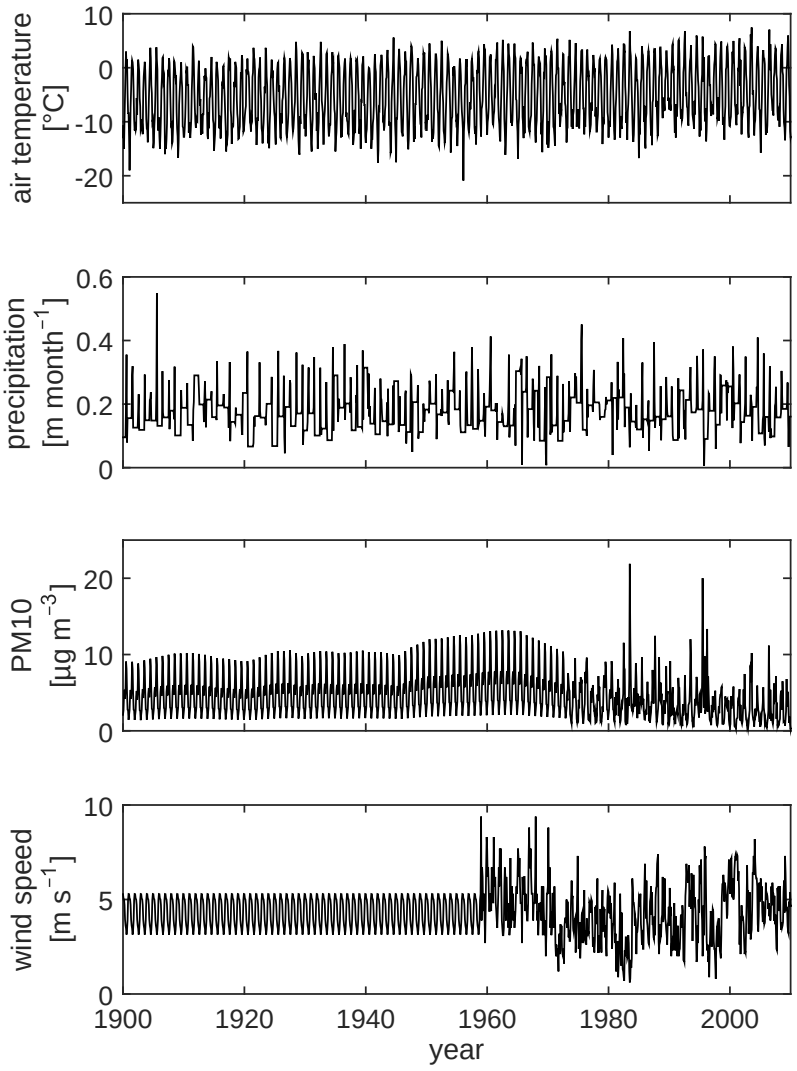

Figure S2: Environmental input parameters on the ice core site. Air temperature, precipitation, PM10, and wind speed in a monthly resolution between January 1900 and December 2010.

Figure S3: Map of Switzerland with the Silvretta glacier (red dot) and the meteorological stations Weissfluhjoch, Davos, Säntis, and Jungfraujoch (blue dots).

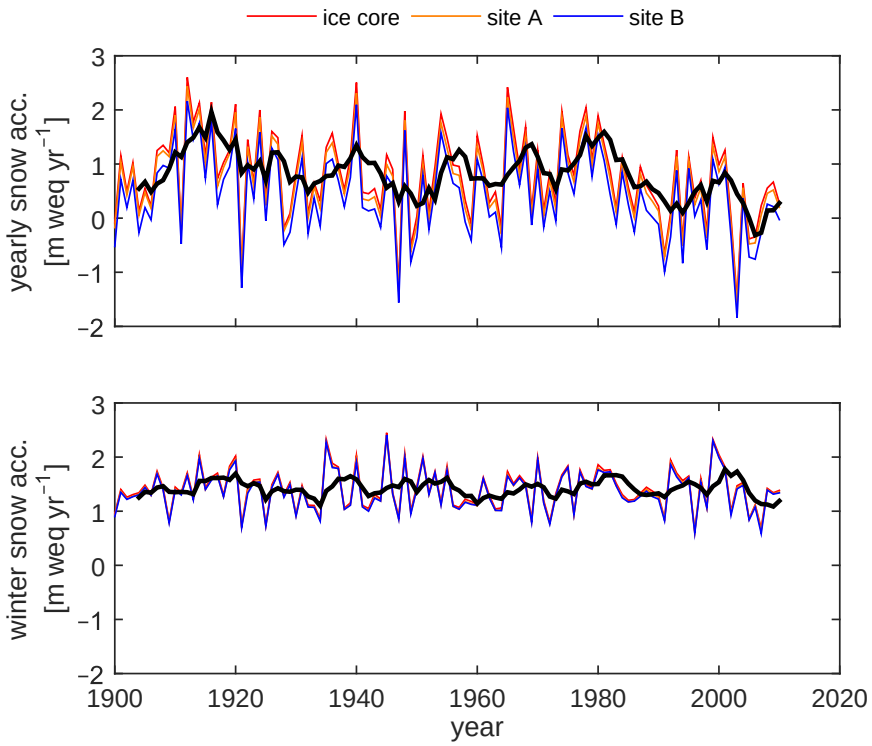

Figure S4: Annual and winter snow accumulation on the ice core site (red line), site A (orange line), and site B (blue line) in meters water equivalent (m weq) per year. A negative snow accumulation indicates snowmelt. The solid black line is the simple moving average of the snow accumulation at the ice core site, with a lag of 5 years. The annual balance is reached in the last summer month; the winter balance in the last winter month. The snow accumulation of the remaining months is calculated by linear interpolation.

The density of the glacier compartments (ρ) increases with depth (d) (Equation (S7)). The fitting parameters X_1, X_2, and X_3 are set to 567, 10, and 350, in the same range as parameters determined for Fiescherhorn glacier in Steinlin et al. [38]. The units of density and depth are $\mathrm{kg\,m^{-3}}$ and m weq, respectively. In addition to the increase of density with depth, the density can increase due to refreezing (see Sections S4.2 and S4.3).

$$\rho = X_1 * (1 - exp(-\frac{1}{X_2} * d)) + X_3 \tag{S7}$$

The porosity (ϕ) of the glacier compartments is calculated as a function of the density of the compartment (ρ, kg $\mathrm{m^{-3}}$) and the density of ice (ρ_{ice}, kg $\mathrm{m^{-3}}$) (Equation (S8)).

$$\phi = 1 - \frac{\rho}{\rho_{\mathrm{ice}}} \tag{S8}$$

The volume fraction of pore air in the compartment is set equal to the porosity. The volume fraction of particles in the compartment depends on the amount of aerosol particles deposited by wet and dry particle deposition during a specific month and the volume of the compartment, which depends on the amount of snow accumulated on the surface and the compartment density. The volume fraction of liquid water is set to 0.09 during summer [14], and zero during winter. The volume fraction of solid ice is then calculated from the volume fractions of the other subcompartments, decreasing during summer due to the increase of the liquid water phase.

The ice temperature in the glacier surface T_{firn} is monthly resolved as a function of depth (Equation (S9)). The temperature in the deep glacier (T_0) is set to 273 K, the amplitude of the temperature (A_{T}) to 10 K, the cycle per time unit (ω) is 1 per 12 months, the thermal diffusivity (α_{T}) is $10^{-6}\,\mathrm{m^2\,s^{-1}}$. z indicates the depth of the glacier compartment, while t indicates the time.

$$T_{\mathrm{firn}} = T_0 + A_{\mathrm{T}} * \exp(-z * \sqrt{\frac{\pi * \omega}{\alpha_{\mathrm{T}}}}) * \sin(2 * \pi * \omega * t - z * \sqrt{\frac{\pi * \omega}{\alpha_{\mathrm{T}}}}) \tag{S9}$$

Other environmental parameters are constant and reported in Table S1. The air height is set to 400 m, a value which is uncertain, but not influential (see Figure S13).

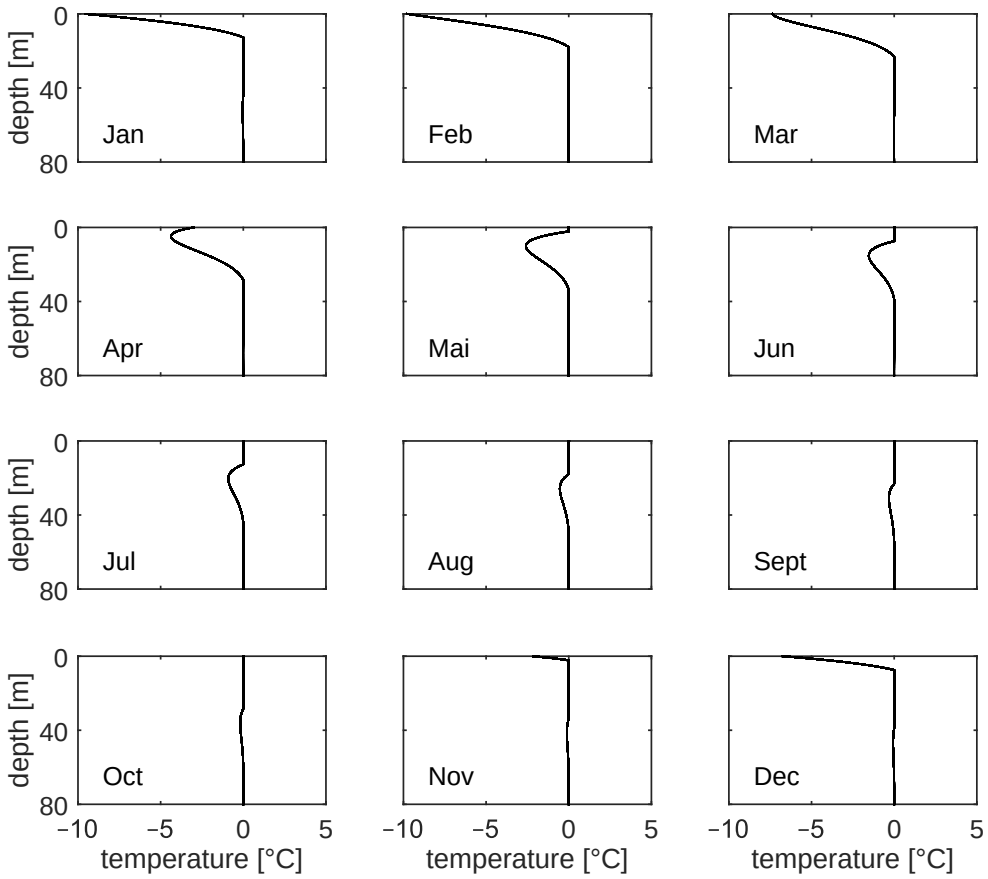

Figure S5: Modeled firn temperature for the twelve months of the year, including the surface freezing during winter.

Table S1: Constant environmental input parameters used in the model.

Parameter	Unit	Value	Reference
Air compartment			
Air height	m	400	
Volume fraction of organic matter in aerosol particles	-	0.2	[12]
Density of aerosol particles	kg m^{-3}	1000	[12]
Dry deposition velocity of aerosols	m h^{-1}	1.8	[9]
Scavenging factor of snow	-	3.2 10^5	[15]
Scavenging factor of rain	-	2 10^5	[24]
Specific surface area of snowflakes	m^2 kg^{-1}	96	[23]
Temperature gradient for elevation correction	°C/100m	0.83	[43]
Glacier compartments			
Volume fraction of liquid water in glacier compartments (summer)	-	0.09	[14]
Volume fraction of organic matter in particles	-	0.2	set equal to aerosols
Density of ice	kg m^{-3}	917	[8]
Density of particles in ice	kg m^{-3}	1000	set equal to aerosols

S4.2 Compartment Setup

The monthly accumulated or melted snow (=change in the local glacier mass balance) (dM_{ice}) dictates the compartment setup (see main text). The compartment setup is different for every site and every month, according to the specific mass balance. During winter, when the mass balance is positive, new compartments are formed on the glacier surface, with dimensions dictated by the mass balance. Let's assume four winter months (months 1–4), with a mass balance $dM_{\text{ice}} = 0.2\,\text{m weq month}^{-1}$. During the four months, four compartments are formed on the glacier surface, each one with dimensions of 0.2 m weq. This unit describes the vertical dimension and is, after being transformed to meters, multiplied with the surface area of the site to calculate the volume of the compartment.

$$\begin{array}{cccc} \text{(month 1)} & \text{(2)} & \text{(3)} & \text{(4)} \\ & & & \begin{bmatrix} 0.2 \\ 0.2 \\ 0.2 \\ 0.2 \end{bmatrix} \\ & & \begin{bmatrix} 0.2 \\ 0.2 \\ 0.2 \end{bmatrix} & \\ & \begin{bmatrix} 0.2 \\ 0.2 \end{bmatrix} & & \\ \begin{bmatrix} 0.2 \end{bmatrix} & & & \end{array} \quad [\text{m weq}]$$

Following the function in Equation (S7), the density of these four compartments increases with depth. The top compartments has the lowest density ($356\,\text{kg m}^{-3}$), which is the density in an average depth of 0.1 m weq.

$$\begin{array}{cccc} \text{(month 1)} & \text{(2)} & \text{(3)} & \text{(4)} \\ & & & \begin{bmatrix} 356 \\ 367 \\ 378 \\ 388 \end{bmatrix} \\ & & \begin{bmatrix} 356 \\ 367 \\ 378 \end{bmatrix} & \\ & \begin{bmatrix} 356 \\ 367 \end{bmatrix} & & \\ \begin{bmatrix} 356 \end{bmatrix} & & & \end{array} \quad [\text{kg m}^{-3}]$$

During summer, the mass balance is negative. This means, material according to the mass balance is lost from the glacier surface, transforms to meltwater, percolates down, and is lost from the glacier column. Therefore, compartments on the surface shrink and are inactivated. Let's assume three summer months, where the mass balance is –0.1 m weq month^{-1}. Every month, 0.1 m weq are lost from the glacier surface. Here are the dimensions of the compartments for the four winter and three summer months.

$$\begin{array}{ccccccc} \text{(month 1)} & \text{(2)} & \text{(3)} & \text{(4)} & \text{(5)} & \text{(6)} & \text{(7)} \\ & & & \begin{bmatrix} 0.2 \\ 0.2 \\ 0.2 \\ 0.2 \end{bmatrix} & \begin{bmatrix} 0.1 \\ 0.2 \\ 0.2 \\ 0.2 \end{bmatrix} & & \\ & & \begin{bmatrix} 0.2 \\ 0.2 \\ 0.2 \end{bmatrix} & & & \begin{bmatrix} 0.2 \\ 0.2 \\ 0.2 \end{bmatrix} & \begin{bmatrix} 0.1 \\ 0.2 \\ 0.2 \end{bmatrix} \\ & \begin{bmatrix} 0.2 \\ 0.2 \end{bmatrix} & & & & & \\ \begin{bmatrix} 0.2 \end{bmatrix} & & & & & & \end{array} \quad [\text{m weq}]$$

The densities of the compartments do not decrease when approaching the surface, leading to a higher compartment density on the glacier surface during summer than during winter.

(month 1)	(2)	(3)	(4)	(5)	(6)	(7)	
			$\begin{bmatrix}356\\367\\378\\388\end{bmatrix}$	$\begin{bmatrix}356\\367\\378\\388\end{bmatrix}$			$[\mathrm{kg\,m^{-3}}]$
		$\begin{bmatrix}356\\367\\378\end{bmatrix}$			$\begin{bmatrix}367\\378\\388\end{bmatrix}$	$\begin{bmatrix}367\\378\\388\end{bmatrix}$	
	$\begin{bmatrix}356\\367\end{bmatrix}$						
$\begin{bmatrix}356\end{bmatrix}$							

Once the dimensions of the compartments in m weq and the densities are defined, we can calculate the dimension of the compartment in meter using Equation (S10), where L_m is the dimension of the compartment in meter, and L_mweq is the dimension of the compartment in meter water equivalent, ρ_wat is the density of water, and ρ the density of the compartment.

$$L_\mathrm{m} = L_\mathrm{mweq} * \rho_\mathrm{wat}/\rho \tag{S10}$$

(month 1)	(2)	(3)	(4)	(5)	(6)	(7)	
			$\begin{bmatrix}0.562\\0.545\\0.529\\0.516\end{bmatrix}$	$\begin{bmatrix}0.281\\0.545\\0.529\\0.516\end{bmatrix}$			[m]
		$\begin{bmatrix}0.562\\0.545\\0.529\end{bmatrix}$			$\begin{bmatrix}0.545\\0.529\\0.516\end{bmatrix}$	$\begin{bmatrix}0.273\\0.529\\0.516\end{bmatrix}$	
	$\begin{bmatrix}0.562\\0.545\end{bmatrix}$						
$\begin{bmatrix}0.562\end{bmatrix}$							

In addition to the mass lost from the surface by the negative mass balance (snowmelt), additional mass is lost from the surface to refreeze in lower compartments. This amount is set to 20% of the mass balance (see Section S4.3 for more information). Therefore, in our example, additional 0.02 m weq are lost from the surface per month. As a consequence, in total, 0.12 m weq are melt on the surface, and percolate down; 0.02 m weq are added to underlying compartments; 0.1 m weq run off as meltwater runoff. In this example, we assume the refreezing to happen uniformly in all compartments, however, in the model, the refreezing meltwater is distributed to the compartments as a function of depth and density (see main text and Section S4.3). The dimensions of the compartments (m weq) are then the following.

(month 1)	(2)	(3)	(4)	(5)	(6)	(7)	
			$\begin{bmatrix}0.2\\0.2\\0.2\\0.2\end{bmatrix}$	$\begin{bmatrix}0.08\\0.207\\0.207\\0.207\end{bmatrix}$			[m weq]
		$\begin{bmatrix}0.2\\0.2\\0.2\end{bmatrix}$			$\begin{bmatrix}0.167\\0.217\\0.217\end{bmatrix}$	$\begin{bmatrix}0.047\\0.227\\0.227\end{bmatrix}$	
	$\begin{bmatrix}0.2\\0.2\end{bmatrix}$						
$\begin{bmatrix}0.2\end{bmatrix}$							

The dimension of the compartment on the glacier surface in the last month (0.047 m weq) is below the cutoff size of 5 cm weq. In order to minimize the number of compartments in the model, a compartment below the cutoff size is inactivated, and its mass is transferred to the underlying compartment, which increases from 0.227 to 0.274 m weq.

(month 1)	(2)	(3)	(4)	(5)	(6)	(7)	
			$\begin{bmatrix}0.2\\0.2\\0.2\\0.2\end{bmatrix}$	$\begin{bmatrix}0.08\\0.207\\0.207\\0.207\end{bmatrix}$			[m weq]
		$\begin{bmatrix}0.2\\0.2\\0.2\end{bmatrix}$			$\begin{bmatrix}0.167\\0.217\\0.217\end{bmatrix}$		
	$\begin{bmatrix}0.2\\0.2\end{bmatrix}$					$\begin{bmatrix}0.274\\0.227\end{bmatrix}$	
$\begin{bmatrix}0.2\end{bmatrix}$							

Except for the compartments on the surface, from where the refreezing meltwater is lost, the refreezing does not change the size of the compartments in meter, as the compartments within the glacier can not increase or decrease in size. However, the refreezing increases the density of the compartments where the meltwater refreezes. We can calculate the new densities using Equation (S11), where L_{mweq} is the compartment dimension in m weq, L_{m} is the compartment dimension in m, and ρ_{wat} is the density of water ($1000\,\mathrm{kg\,m^{-3}}$, or here unit-wise more correct: $\mathrm{kg\,m^{-2}\,m\,weq^{-1}}$). In addition, due to solar radiation, the density of the surface compartment increases by 20% in each summer month (not shown here).

$$\rho = L_{\mathrm{mweq}} * \rho_{\mathrm{wat}} / L_{\mathrm{m}} \tag{S11}$$

(month 1)	(2)	(3)	(4)	(5)	(6)	(7)	
			$\begin{bmatrix}356\\367\\378\\388\end{bmatrix}$	$\begin{bmatrix}356\\380\\391\\401\end{bmatrix}$			$[\mathrm{kg\,m^{-3}}]$
		$\begin{bmatrix}356\\367\\378\end{bmatrix}$			$\begin{bmatrix}380\\410\\421\end{bmatrix}$		
	$\begin{bmatrix}356\\367\end{bmatrix}$					$\begin{bmatrix}429\\440\end{bmatrix}$	
$\begin{bmatrix}356\end{bmatrix}$							

This compartment setup leads to a monthly varying number of compartments in the system. As the setup depends on the local mass balance, the number of compartments is individual for every site on the glacier surface. Figure S6 illustrates the number of compartments between 1900 and 2010 (1332 months) on the ice core site, site A, and site B.

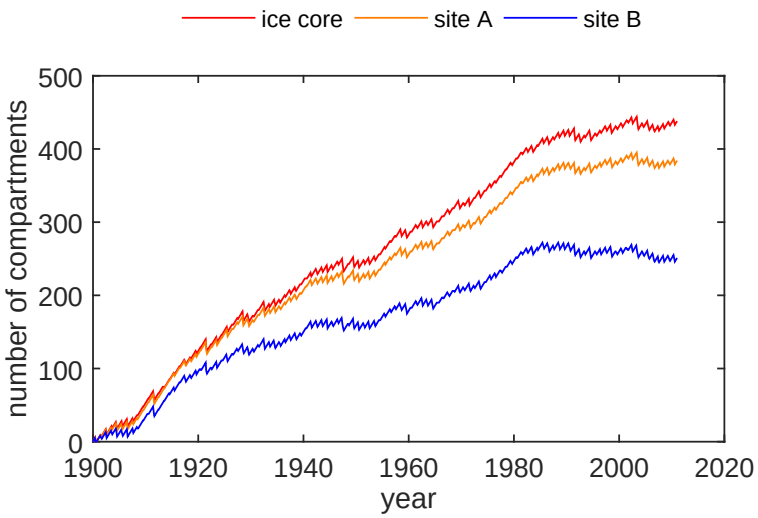

Figure S6: Number of compartments in the system between 1900 and 2010 on the ice core site, site A, and site B. On all sites, the number of compartments increases until the 1980s, when snow accumulation decreases. As a consequence, the number of compartments remains constant (ice core site, site A) or decreases (site B).

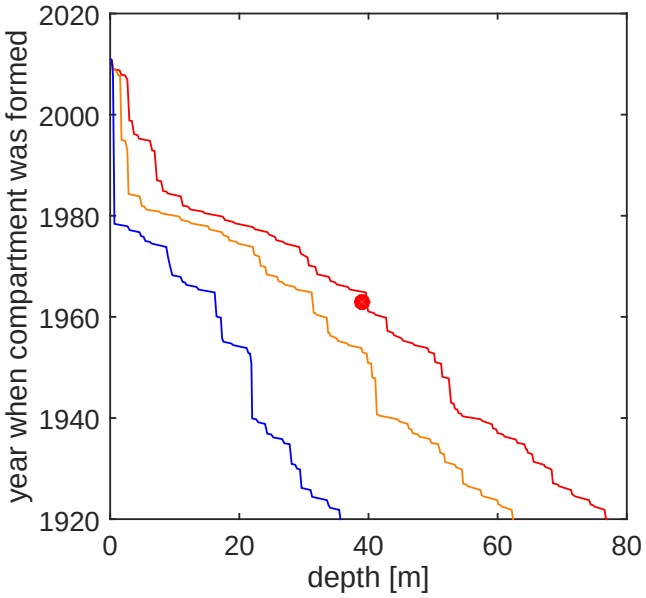

Figure S7: Modeled age-depth relationship as calculated from the snow accumulation and meltwater refrezing on the ice core site (red line), site A (yellow line), and site B (blue line). Age-depth relationship derived by isotopic tritium (^{3}H) dating (red dot) [31, 30]. The smaller snow accumulation on site B leads to an older age of compartments at a smaller depth. The ice formed in the 1970s is located at 30–40 m depth (ice core), 30 m depth (site A), and 10 m depth (site B).

S4.3 Meltwater Percolation and Runoff

Functions and parameters of meltwater processes are selected in a way that modeled and measured [31] density profiles in the ice core are similar (Figure S8). As described in the main text and above, the amount of snow melt at the glacier surface and lost from the glacier as runoff is equal to the total change in local mass balance (dM_{ice}, $\text{m weq}\,\text{month}^{-1}$). Snowmelt only occurs during summer when dM_{ice} is negative. Snowmelt processes are active down to a depth of 15 m weq (d_{max}).

The amount of meltwater lost from individual glacier compartments as runoff ($U_{\text{w,run}}$) is inversely correlated to depth (d) (Equation (S12)). The distribution of meltwater runoff to the glacier compartments ($U_{\text{w,run,key}}$, a value between 0 and 1) is first calculated as a function of depth, relative to the maximum depth where the process is active (d_{max}). Then, $U_{\text{w,run,key}}$ is multiplied by dM_{ice} and divided by its sum, so that the sum of meltwater lost from the glacier compartments corresponds to dM_{ice} (Equation (S13)). The unit of $U_{\text{w,run}}$ is $\text{m weq}\,\text{month}^{-1}$.

$$U_{\text{w,run,key}} = 1 - \frac{d}{d_{\text{max}}} \tag{S12}$$

$$U_{\text{w,run}} = U_{\text{w,run,key}} * \frac{-dM_{\text{ice}}}{\sum U_{\text{w,run,key}}} \tag{S13}$$

The amount of snow melt at the glacier surface for refreezing in the glacier compartments is set to 20% of dM_{ice}. The amount of meltwater refreezing in individual glacier compartments ($U_{\text{w,freez}}$) is a function of compartment density (ρ) and depth (d) (Equation (S14)), where depth is weighted to be twice as important as density. The distribution-parameter ($U_{\text{w,freez,key}}$) is then multiplied by $0.2 * -dM_{\text{ice}}$ and divided by its sum, so that the total amount of refreezing meltwater is 20% of dM_{ice} (Equation (S15)). The unit of $U_{\text{w,freez}}$ is $\text{m weq}\,\text{month}^{-1}$.

$$U_{\text{w,freez,key}} = \frac{\rho}{\rho_{\text{max}}} + 2 * (1 - \frac{d}{d_{\text{max}}}) \tag{S14}$$

$$U_{\text{w,freez}} = U_{\text{w,freez,key}} * \frac{0.2 * -dM_{\text{ice}}}{\sum U_{\text{w,freez,key}}} \tag{S15}$$

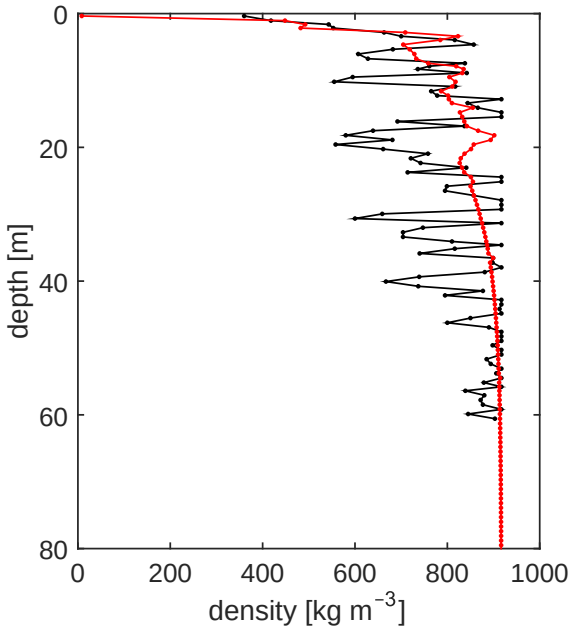

Figure S8: Modeled (red line) and measured (black line [31]) density profiles in the ice core. The modeled density profile is averaged over the sample depth.

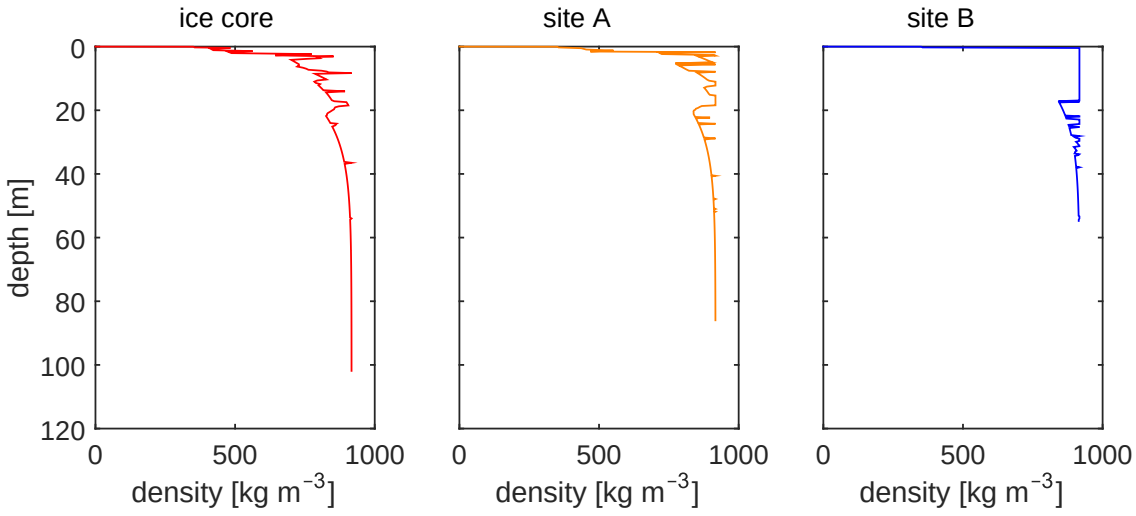

Figure S9: Modeled density profiles on the ice core site (red line, left plot), site A (orange line, middle plot), and site B (blue line, right plot). In contrast to Figure S8, the density profiles are not averaged over the sample depth. The stronger melt on sites A and B leads to strong melt layers (high densities) in the upper 20 m.

S4.4 Particle Percolation and Runoff

Similar to the meltwater processes, we select functions and parameters of particle processes by comparing the modeled black carbon profile with the black carbon profile measured in the ice core [31] (Figure S10). For this, we assume a black carbon content of the aerosol particles in the model of 2.4%, according to PM10 and black carbon measurements from Jungfraujoch [11]. Modeled and measured black carbon profiles are similar.

The fraction of particles washed out from a glacier compartment and leaving the glacier as particle runoff ($f_{\mathrm{p,run}}$) is a function of compartment density (ρ) and depth (d), with increasing runoff when density and depth are low (Equation (S16)). Again, depth is weighted to be twice as important as density. The parameter $f_{\mathrm{p,run}}$ is unitless, as this is a fraction of the particles that are present in a specific glacier compartment. This fraction is set to reach a maximum of 0.02, therefore, $f_{\mathrm{p,run,key}}$ is multiplied by 0.02 and divided by its maximum value ($f_{\mathrm{p,run,key,max}}$) (Equation (S17)). In the model, particles are washed out from a glacier compartment to leave the glacier as particle runoff down to a depth of 10 m weq.

$$f_{\mathrm{p,run,key}} = (1 - \frac{\rho}{\rho_{\mathrm{max}}}) + 2 * (1 - \frac{d}{d_{\mathrm{max}}}) \tag{S16}$$

$$f_{\mathrm{p,run}} = f_{\mathrm{p,run,key}} * \frac{0.02}{f_{\mathrm{p,run,key,max}}} \tag{S17}$$

The fraction of particles washed out from a glacier compartment and being relocated with percolating meltwater ($f_{\mathrm{p,perc}}$) is also a function of compartment density and depth (Equation S18). Again, this parameter is unitless, as it describes a fraction of the particles in the glacier compartment, and its maximum value is set to 0.01 (Equation S19). In the model, particles are washed out from a glacier compartment to be relocated down to a depth of 10 m weq.

$$f_{\mathrm{p,perc,key}} = (1 - \frac{\rho}{\rho_{\mathrm{max}}}) + 2 * (1 - \frac{d}{d_{\mathrm{max}}}) \tag{S18}$$

$$f_{\mathrm{p,perc}} = f_{\mathrm{p,perc,key}} * \frac{0.01}{f_{\mathrm{p,perc,key,max}}} \tag{S19}$$

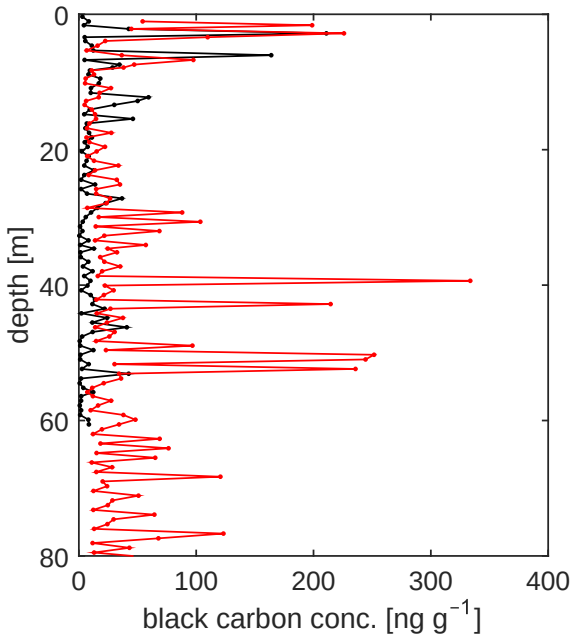

Figure S10: Modeled (red line) and measured (black line [31]) black carbon profile in the ice core, using a black carbon content of aerosols of 2.4% (red line). Modeled and measured profiles are averaged over the sample depth.

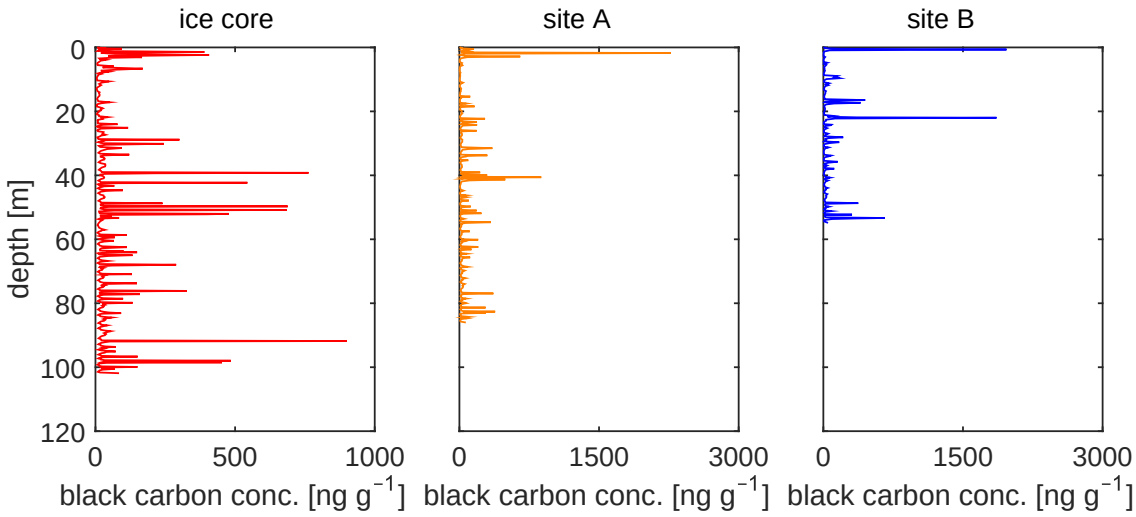

Figure S11: Modeled black carbon profiles on the ice core site (red line, left plot), site A (orange line, middle plot), and site B (blue line, right plot). In contrast to Figure S10, the profiles are not averaged over depth, but correspond to the individual compartments. The stronger melt on sites A and B leads to stronger enrichment of particles (higher concentrations) in the surface layers

S5 Input of Chemicals into the System

The maximum PCB emission scenario by Breivik et al. was used as input to the global chemical fate model BETR Research [7, 44]. BETR Research includes 288 regions on a 15° x 15° resolution, with each region containing seven compartments: upper air, lower air, vegetation, fresh water, ocean water, soil, and freshwater sediment. The upper air compartment describes the free troposphere, while the lower air compartment represents the planetary boundary layer. We assume an air mix of 20% tropospheric air and 80% boundary layer air reaching Silvretta glacier during summer, and pure tropospheric air reaching Silvretta glacier during winter. The mixing ratio during summer was estimated from seasonal variations in sulfate concentration in aerosol particles at Jungfraujoch, compared to sulfate concentrations in the Swiss lowlands. For more information please refer to the Supporting Information of Steinlin et al. [38].

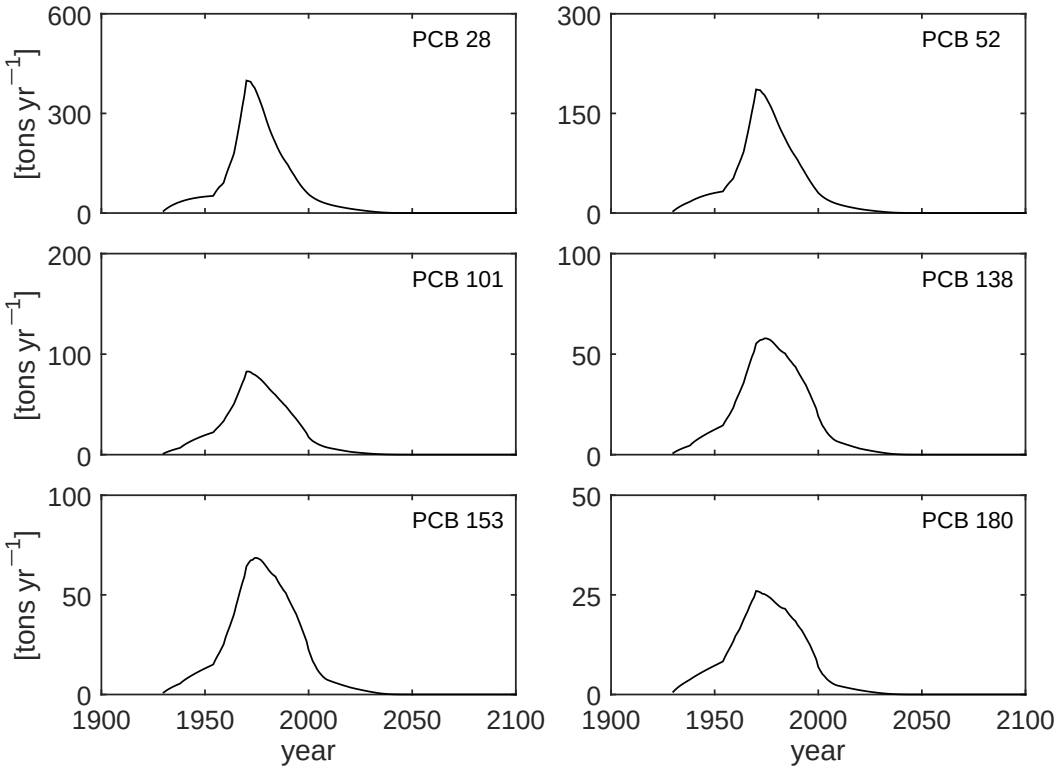

Figure S12: Global emissions of the PCB congeners 28, 52, 101, 138, 153, and 180, as estimated in the maximum emission scenario of Breivik et al. [7].

S6 Physicochemical and Kinetic Properties of PCBs

Physicochemical properties of the six indicator PCBs are shown in Table S2.

S6.1 Basic Partition Coefficients

The partition coefficients octanol–water (K_{ow}), air–water (K_{aw}), and octanol–air (K_{oa}) are adjusted to temperature using the van't Hoff equation (Equations (S20)–(S22)), where dU is the energy of phase change ($\mathrm{J\,mol^{-1}}$), R the gas constant ($8.31\,\mathrm{J\,mol^{-1}\,K^{-1}}$), T_{c} the temperature of the property data (K), and T the temperature in a specific compartment (K).

$$K_{\mathrm{ow}}(T) = K_{\mathrm{ow}}(T_{\mathrm{c}}) * exp(\frac{dU_{\mathrm{ow}}}{R} * (\frac{1}{T_{\mathrm{c}}} - \frac{1}{T})) \tag{S20}$$

$$K_{\mathrm{aw}}(T) = K_{\mathrm{aw}}(T_{\mathrm{c}}) * exp(\frac{dU_{\mathrm{aw}}}{R} * (\frac{1}{T_{\mathrm{c}}} - \frac{1}{T})) \tag{S21}$$

$$K_{\mathrm{oa}}(T) = K_{\mathrm{oa}}(T_{\mathrm{c}}) * exp(\frac{dU_{\mathrm{oa}}}{R} * (\frac{1}{T_{\mathrm{c}}} - \frac{1}{T})) \tag{S22}$$

S6.2 Particle–Air Partitioning

The aerosol particle–air (in the atmosphere, $K_{\mathrm{pa,air}}$) and particle–pore air (in the glacier, $K_{\mathrm{pa,gla}}$) partition coefficients are calculated from the temprature-adjusted K_{oa} and the fraction of organic matter in the particle (f_{om}) as described by Harner et al. [19] (Equation (S23)). The factor 10^9 transforms the units of $K_{\mathrm{pa,dim}}$ from $\mathrm{m^3\,\mu g^{-1}}$ to $\mathrm{m^3\,kg^{-1}}$. The partition coefficient with dimensions ($K_{\mathrm{pa,dim}}$) is then transformed to the unitless partition coefficients using the density of aerosols (ρ_{aer}, $\mathrm{kg\,m^{-3}}$) and particles (ρ_{par}, $\mathrm{kg\,m^{-3}}$) (Equations (S24)–(S25), Table S2).

Table S2: Physicochemical and kinetic properties of the PCB congeners 28, 52, 101, 138, 153, and 180. For more details please refer to the text. [a]wet K_{ow}.

Parameter	Unit	PCB 28	PCB 52	PCB 101	PCB 138	PCB 153	PCB 180	Ref.
molar mass	$\mathrm{g\,mol^{-1}}$	257.5	292.0	326.4	360.9	360.9	395.3	
log K_{ow}[a]	[−]	5.66	5.95	6.38	7.19	6.86	7.15	[33]
log K_{aw}	[−]	-1.93	-1.96	-2.08	-1.97	-2.13	-2.51	[33]
log K_{oa}	[−]	7.86	8.22	8.83	9.67	9.45	10.17	[33]
dU_{ow}	$\mathrm{kJ\,mol^{-1}}$	-26.6	-27.5	-19.3	-22.2	-26.6	-26.1	[33]
dU_{aw}	$\mathrm{kJ\,mol^{-1}}$	51.8	53.8	65.2	64.7	68.2	69.0	[33]
dU_{oa}	$\mathrm{kJ\,mol^{-1}}$	-78.4	-81.3	-84.4	-86.9	-97.8	-95.2	[33]
A	[−]	0	0	0	0	0	0	[41]
B	[−]	0.055	0	0	0	0	0	[41]
log K_{ha}	[−]	7.90	8.14	8.87	9.78	9.59	10.42	[1]
$k_{\mathrm{air,sec}}$	$10^{-12}\,\mathrm{cm^3\,molecule^{-1}\,s^{-1}}$	1.23	0.74	0.45	0.27	0.27	0.16	[4]
$k_{\mathrm{pho,mean}}$	$10^{-5}\,\mathrm{h^{-1}}$	7.9	7.9	7.9	7.9	7.9	7.9	[25]
$E_{\mathrm{a,air}}$	$\mathrm{kJ\,mol^{-1}}$	15.0	15.0	15.0	15.0	15.0	15.0	[5]

$$K_{\mathrm{pa,dim}} = 10^9 * 10^{(\log K_{\mathrm{oa}} + \log f_{\mathrm{om}} - 11.91)} \tag{S23}$$

$$K_{\mathrm{pa,air}} = K_{\mathrm{pa,dim}} * \rho_{\mathrm{aer}} \tag{S24}$$

$$K_{\mathrm{pa,gla}} = K_{\mathrm{pa,dim}} * \rho_{\mathrm{par}} \tag{S25}$$

S6.3 Snow Surface–Air Partitioning

The snow surface–air partition coefficient is calculated from the hexadecane–air partition coefficient (K_{ha}), electron acceptor property (A), and electron donor property (B) according to Roth et al. [32] (Equation (S26)). $K_{\mathrm{ca,dim,c}}$ has units of $\mathrm{m^3\,m^{-2}}$ and is valid for –6.8 °C.

$$\log K_{\mathrm{ca,dim,c}} = 0.639 * \log K_{\mathrm{ha}} + 3.53 * A + 3.38 * B - 6.85 \tag{S26}$$

Temperature dependence is calculated using Equation (4) in Goss and Schwarzenbach [17] (Equation (S27)), where T_{cc} is –6.8 °C, T_{av} is the average temperature in the considered temperature range, T is the actual temperature in a glacier compartment, and ΔH the enthalpy of sorption.

$$K_{\mathrm{ca,dim}} = K_{\mathrm{ca,dim,c}} * \exp\left(\frac{-\Delta H + R * T_{\mathrm{av}}}{R} * \left(\frac{1}{T} - \frac{1}{T_{\mathrm{cc}}}\right)\right) \tag{S27}$$

The enthalpy of sorption (ΔH) is assumed to be constant, and is calculated as a function of $K_{\mathrm{ca,dim,c}}$, similar to Equation (11) in Goss and Schwarzenbach [17] (Equation (S28)). In Equation (S28), $K_{\mathrm{ca,dim,c}}$ is valid at 20 °C, therefore, we adapted this equation for the use of $K_{\mathrm{ca,dim,c}}$ at –6.8 °C (Equation (S29)).

$$\Delta H = -5.26 * \ln K_{\mathrm{ca,dim,c}} - 112 \tag{S28}$$

$$\Delta H = -4.32 * \ln K_{\mathrm{ca,dim,c}} - 92.4 \tag{S29}$$

The unitless partition coefficients snowflake–air (K_{sa}, in the atmosphere) and glacier ice–pore air (K_{ga}, in the glacier) are then calculated using the snow surface area of snowflakes (A_{sf}) and ice (A_{ice}) in the specific compartment and the density of ice (ρ_{ice}) (Equations (S30)–(S31)). While A_{sf} has a constant value of $96\,\mathrm{m^2\,kg^{-1}}$ (Table S1), A_{ice} is a function of density up to compartment densities of $500\,\mathrm{kg\,m^{-3}}$ (Equation (S32), [10]), and set to a constant value of $10\,\mathrm{m^2\,kg^{-1}}$ in compartments with densities above $500\,\mathrm{kg\,m^{-3}}$.

$$K_{\mathrm{sa}} = K_{\mathrm{ca,dim}} * A_{\mathrm{sf}} * \rho_{\mathrm{ice}} \tag{S30}$$

$$K_{\mathrm{ga}} = K_{\mathrm{ca,dim}} * A_{\mathrm{ice}} * \rho_{\mathrm{ice}} \tag{S31}$$

$$A_{\mathrm{gla}} = -313.17 * \ln \rho + 160.1 \tag{S32}$$

S6.4 Degradation Rate Constants

The degradation rate constant in air (k_{air}) is calculated from the second-order rate constant for the degradation with hydroxyl radicals ($k_{\mathrm{air,sec}}$, $\mathrm{cm^3\,molecule^{-1}\,s^{-1}}$, Table S2) and the concentration of hydroxyl radicals in the atmosphere (C_{OH}, $\mathrm{molecules\,cm^{-3}}$) (Equation (S33)). The second-order rate constant is calculated from the degree of chlorination (N_{Cl}) of the PCB congeners using a regression presented in Anderson and Hites [4] (Equation (S34)). The concentration of hydroxyl radicals is seasonally resolved, varying between $1.4\,10^5$ and $25.1\,10^5$ $\mathrm{molecules\,cm^{-3}}$, and is valid for a latitude of 44° N and a pressure of 700 hPa [37]. The degradation rate constant is adjusted to temperature using the two-point Arrhenius equation (Equation (S35)), where $E_{\mathrm{a,air}}$ is the activation energy of the rate

constant in air ($\mathrm{J\,mol^{-1}}$, Table S1), R is the gas constant ($8.31\,\mathrm{J\,mol^{-1}\,K^{-1}}$), T_c the temperature of the property data (K), and T the air temperature (K).

$$k_\mathrm{air} = k_\mathrm{air,sec} * C_\mathrm{OH} \tag{S33}$$

$$\log k_\mathrm{air,sec} = -0.22 * N_\mathrm{Cl} - 11.25 \tag{S34}$$

$$k_\mathrm{air}(T) = k_\mathrm{air}(T_\mathrm{c}) * exp(-\frac{E_\mathrm{a,air}}{R} * (\frac{1}{T} - \frac{1}{T_\mathrm{c}})) \tag{S35}$$

The photochemical degradation rate constant reported in Table S2 corresponds to a halflife of approximately one year [25]. We assume this rate constant to be the average rate constant in the model, and adapt it to seasonal changes in radiation using a factor of 1.5, according to the seasonal variation in radiation at Weissfluhjoch [39]. This factor increases the rate constant during the summer months and decreases the rate constant during the winter months. Photochemical degradation is occurring only in the top glacier compartment, and only in the top 15 cm of the compartment [18]. This means, the degradation rate constant is decreased if the surface compartment is higher than 15 cm. We assume that only the fraction of chemicals in the solid ice subcompartment can be degraded photochemically.

S6.5 Molecular Diffusivity

Molecular diffusivity in air ($d_\mathrm{diff,air}$, $\mathrm{m^2\,s^{-1}}$) is a function of the molar mass (M) ($\mathrm{g\,mol^{-1}}$) according to Schwarzenbach et al. [35] (Equation (S36)).

$$d_\mathrm{diff,air} = \frac{1.55}{M^{0.65}}/10000 \tag{S36}$$

S6.6 Fugacity Capacities

The fugacity capacities of the pure phases (Z-values) are calculated as a function of the partition coefficients [24]. Equations (S37)–(S38) illustrate the calculation of the fugacity capacities in pure air (Z_a) and pure water (Z_w). The fugacity capacities of the compartments are then calculated as a function of the fugacity capacities of the subcompartments (pure phases) and the volume fractions of the subcompartments in the compartment. For more information on fugacity capacities see Mackay [24].

$$Z_\mathrm{a} = \frac{1}{R * T} \tag{S37}$$

$$Z_\mathrm{w} = \frac{Z_\mathrm{a}}{K_\mathrm{aw}} \tag{S38}$$

S7 Chemical Fate Processes

The D-values used in the system of differential equations in Equation (S1) are calculated by combining the D-values of every single process accounted for in the model.

S7.1 Air Advection

The D-value of air advection (D_{airadv}) is calculated by multiplying the amount of air flowing in and out of the system (G_{air}, $\mathrm{m^3\,month^{-1}}$) and the fugacity capacity of the air compartment (Z_{air}, $\mathrm{mol\,Pa^{-1}\,m^{-3}}$) (Equation (S39)).

$$D_{\mathrm{adv,air}} = G_{\mathrm{air}} * Z_{\mathrm{air}} \tag{S39}$$

S7.2 Degradation

The D-values of degradation by OH-radicals in air ($D_{\mathrm{deg,air}}$) and photochemical degradation in the glacier surface ($D_{\mathrm{deg,gla}}$) are shown in Equations (S40)–(S41). The following parameters are used in the equations: degradation rate constant in air (k_{air}, $\mathrm{month^{-1}}$), degradation rate constant in the glacier surface (k_{pho}, $\mathrm{month^{-1}}$), volumes of air and glacier surface active for photochemical degradation (V_{air} and V_{pho}, $\mathrm{m^3}$), and the fugacity capacities of the subcompartments air and ice (Z_{a}, Z_{ice}, $\mathrm{mol\,Pa^{-1}\,m^{-3}}$). The use of Z_{ice} here means that only the fraction of chemicals in the solid ice subcompartment is transformed by photochemical degradation.

$$D_{\mathrm{deg,air}} = k_{\mathrm{air}} * V_{\mathrm{air}} * Z_{\mathrm{a}} \tag{S40}$$

$$D_{\mathrm{deg,gla}} = k_{\mathrm{pho}} * V_{\mathrm{pho}} * Z_{\mathrm{ice}} \tag{S41}$$

S7.3 Deposition

The D-values of deposition from the atmosphere to the glacier surface are shown in Equations (S42)–(S46). Dry particle deposition (dp), wet particle deposition (wp), and wet gaseous deposition (wg). While $D_{\mathrm{dep,wp,loss}}$, and $D_{\mathrm{dep,wg,loss}}$ are losses from the system, occurring during summer, $D_{\mathrm{dep,dp}}$, $D_{\mathrm{dep,wp}}$, and $D_{\mathrm{dep,wg}}$ transfer chemical from the atmosphere to the glacier, with $D_{\mathrm{dep,dp}}$ being active during winter and summer, and $D_{\mathrm{dep,wp}}$ and $D_{\mathrm{dep,wg}}$ being active only during winter. The following parameters are used in the equations: particle deposition rate (U_{aer}, $\mathrm{m\,month^{-1}}$), surface area of glacier sections (A_{gla}, $\mathrm{m^2}$), fugacity capacities of the subcompartments aerosol particles, snowflakes, and raindrops (Z_{aer}, Z_{sf}, Z_w, $\mathrm{mol\,Pa^{-1}\,m^{-3}}$), precipitation to the glacier surface (winter) (U_{snow}, $\mathrm{m\,weq\,month^{-1}}$), precipitation as direct runoff (summer) (U_{rain}, $\mathrm{m\,weq\,month^{-1}}$), scavenging factor of snow (winter) or rain (summer) (Q_{snow} and Q_{rain}, unitless), and the volume fraction of aerosol particles in the atmosphere (f_{aer}, unitless).

$$D_{\mathrm{dep,dp}} = U_{\mathrm{aer}} * A_{\mathrm{gla}} * f_{\mathrm{aer}} * Z_{\mathrm{aer}} \tag{S42}$$

$$D_{\mathrm{dep,wp}} = U_{\mathrm{snow}} * Q_{\mathrm{snow}} * A_{\mathrm{gla}} * f_{\mathrm{aer}} * Z_{\mathrm{aer}} \tag{S43}$$

$$D_{\mathrm{dep,wp,loss}} = U_{\mathrm{rain}} * Q_{\mathrm{rain}} * A_{\mathrm{gla}} * f_{\mathrm{aer}} * Z_{\mathrm{aer}} \tag{S44}$$

$$D_{\mathrm{dep,wg}} = U_{\mathrm{snow}} * A_{\mathrm{gla}} * Z_{\mathrm{sf}} \tag{S45}$$

$$D_{\mathrm{dep,wg,loss}} = U_{\mathrm{snow}} * A_{\mathrm{gla}} * Z_{\mathrm{w}} \tag{S46}$$

S7.4 Wind Pumping

Dry gaseous deposition and revolatilization between the atmosphere and the glacier surface as well as between the top and the second glacier compartments are described as advection due to wind-pumping [26]. The D-value of this exchange ($D_{\mathrm{adv,airgla}}$) is a function of the mass transfer coefficient from the atmosphere to the glacier (U_{airgla}) and the mass transfer coefficient from the glacier to the atmosphere (U_{glaair}), as well as the area of the glacier section (A_{gla}), and the fugacity capacity of the air (Z_{a}) and the pore air (Z_{poreair}) (Equation (S47)).

$$D_{\mathrm{adv,airgla}} = \frac{1}{\frac{1}{U_{\mathrm{airgla}} * A_{\mathrm{gla}} * Z_{\mathrm{a}}} + \frac{1}{U_{\mathrm{glaair}} * A_{\mathrm{gla}} * Z_{\mathrm{poreair}}}} \tag{S47}$$

The mass transfer coefficient from the atmosphere to the glacier (U_{airgla}) is a function of wind speed (U_{wind}, $\mathrm{m\,month^{-1}}$) and the aerodynamic roughness length on the glacier (z_0, m), which is set to 0.023 m, an average between values reported for snow and ice [16] (Equation (S48)).

$$U_{\mathrm{airgla}} = 0.4^2 * U_{\mathrm{wind}} * \frac{1}{\ln(\frac{10}{z_0}) * \ln(\frac{2}{z_0})} \tag{S48}$$

The mass transfer coefficient from the glacier to the atmosphere (U_{glaair}) is a function of permeability (P, $\mathrm{m^2}$), the air viscosity (μ, Pa s), the pressure amplitude (p_0, Pa), and the depth of the compartment (d, m) (Equation (S49)).

$$U_{\mathrm{glaair}} = \frac{P}{\mu} * \frac{p_0}{\ln 2 * d} \tag{S49}$$

Permeability is calculated from open porosity (ϕ_{open}) (Equation (S50)), which is calculated from total porosity (ϕ_{tot}) and closed porosity (ϕ_{closed}) (Equation (S51)), where the latter is estimated from the total porosity using the Schwander relationship [34, 2] (Equation (S52)), using a pore close off density of 830 $\mathrm{kg\,m^{-3}}$ [8].

$$P = 10^{7.7} * \phi_{\mathrm{open}}^{3.4} \tag{S50}$$

$$\phi_{\mathrm{open}} = \phi_{\mathrm{tot}} - \phi_{\mathrm{closed}} \tag{S51}$$

$$\phi_{\mathrm{closed}} = \begin{cases} \phi_{\mathrm{tot}} * exp(75 * (\frac{\rho}{830} - 1)) & \text{if } \rho < 830, \\ \phi_{\mathrm{tot}} & \text{if } \rho \geq 830. \end{cases} \tag{S52}$$

The pressure amplitude (p_0) is calculated as a function of the density of air (ρ_{air}, $\mathrm{kg\,m^{-3}}$), the wind speed (U_{wind}, $\mathrm{m\,month^{-1}}$), the surface roughness amplitude (A_{sr}, m), and the surface roughness wavelength (λ, m) (Equation (S53)). The surface roughness amplitude is calculated from the aerodynamic roughness length (z_0) [26, 36] (Equation (S54)), while the surface roughness wavelength is set to 10 m.

$$p_0 = \frac{3 * \rho_{\mathrm{air}} * U_{\mathrm{wind}}^2 * A_{\mathrm{sr}}}{\lambda} \tag{S53}$$

$$A_{\mathrm{sr}} = z_0 * 30 \tag{S54}$$

S7.5 Molecular Diffusion

Exchange between the second and all the lower glacier compartments is described by molecular diffusion (D_{diff}) (Equation (S55)), where diffusion between compartment i and compartment j is a function of the mass transfer coefficient (U_{gla}, $\text{m}\,\text{month}^{-1}$), the area of the glacier section (A_{gla}, m^2) and the fugacity capacity of the pore air (Z_{poreair}, $\text{mol}\,\text{Pa}^{-1}\,\text{m}^{-3}$). The mass transfer coefficient is calculated from the effective diffusivity in pore air ($d_{\text{diff,eff}}$, m^2 month^{-1}) and the size of the compartment (L_{m}, m) (Equation (S56)). The effective diffusivity is a function of the diffusivity in air and the volume fraction of pore air in the compartment (f_{poreair}, unitless) (Equation (S57)) [27].

$$D_{\text{diff}} = \frac{1}{\frac{1}{U_{\text{gla},i} * A_{\text{gla}} * Z_{\text{poreair},i}} * \frac{1}{U_{\text{gla},j} * A_{\text{gla}} * Z_{\text{poreair},j}}} \tag{S55}$$

$$U_{\text{gla}} = \frac{d_{\text{diff,eff}}}{0.5 * L_{\text{m}}} \tag{S56}$$

$$d_{\text{diff,eff}} = d_{\text{diff,air}} * f_{\text{poreair}}^{4/3} \tag{S57}$$

S7.6 Meltwater Processes

Chemicals can percolate through the glacier column or leave the glacier with meltwater. The D-values of percolating meltwater (D_{meltflux}) and meltwater runoff ($D_{\text{meltrunoff}}$) are calculated from the meltwater flux (U_{meltflux} and $U_{\text{meltrunoff}}$, $\text{m}\,\text{month}^{-1}$), the area of the glacier section (A_{gla}, m^2), and the fugacity capacity of the pore water (Z_{w}, $\text{mol}\,\text{Pa}^{-1}\,\text{m}^{-3}$) (Equations (S58)–(S59)).

$$D_{\text{meltflux}} = U_{\text{meltflux}} * A_{\text{gla}} * Z_{\text{w}} \tag{S58}$$

$$D_{\text{meltrunoff}} = U_{\text{meltrunoff}} * A_{\text{gla}} * Z_{\text{w}} \tag{S59}$$

S7.7 Particle Processes

The D-values of percolating particles (D_{partflux}) and particle runoff ($D_{\text{partrunoff}}$) are calculated as a function of the particle flux (U_{partflux} and $U_{\text{partrunoff}}$, $\text{m}\,\text{month}^{-1}$), the area of the glacier section (A_{gla}, m^2), and the fugacity capacity of the particles (Z_{par}, $\text{mol}\,\text{Pa}^{-1}$ m^{-3}) (Equations (S60)–(S61)).

$$D_{\text{partflux}} = U_{\text{partflux}} * A_{\text{gla}} * Z_{\text{par}} \tag{S60}$$

$$D_{\text{partrunoff}} = U_{\text{partrunoff}} * A_{\text{gla}} * Z_{\text{par}} \tag{S61}$$

S8 Sensitivity and Uncertainty Analysis

The following parameters were included in the sensitivity and uncertainty analysis:

1. octanol–water partition coefficient (confidence factor (cf)= 1.1 on log value)
2. air–water partition coefficient (cf= 1.1 on log value)
3. octanol–air partition coefficient (cf= 1.1 on log value)
4. energy of phase change octanol–water (cf= 1.2)
5. energy of phase change air–water (cf= 1.2)
6. energy of phase change octanol–air (cf= 1.2)
7. hexadecane–air partition coefficient (cf= 1.1 on log value)
8. electron acceptor properties (cf= 1.5)
9. electron donor properties (cf= 1.5)
10. degradation rate constant in air (cf= 3)
11. OH radical concentration in air (cf= 1.5)
12. degradation rate constant in water (not used in this model version)
13. degradation rate constant in glacier surface (cf= 10)
14. activation energy of degradation rate constant in air (cf= 1.2)
15. activation energy of degradation rate constant in water (not used in this model version)
16. factor to adjust the photochemical degradation rate to seasonal changes in radiation (cf= 1.5)
17. depth to which photochemical degradation is active (cf= 3)
18. surface area of glacier site (cf= 2)
19. height of air compartment (cf= 3)
20. volume fraction of aerosol particles in the atmosphere (cf= 1.5)
21. volume fraction of liquid water in glacier compartments (cf= 2)
22. volume fraction of organic matter in aerosol particles (cf= 1.5)
23. volume fraction of organic matter in particles in glacier (cf= 1.5)
24. density of aerosol particles (cf= 1.5)
25. density of particles in glacier (cf= 1.5)
26. specific surface area of snowflakes (cf= 1.2)
27. specific surface area of snow/ice in glacier (cf= 2)

28. particle deposition rate (cf= 3)
29. scavenging factor of rain (cf= 5)
30. scavenging factor of snow (cf= 5)
31. air temperature (cf= 1.02)
32. glacier temperature (cf= 1.2)
33. temperature gradient for elevation correction (cf= 1.2)
34. monthly precipitation (cf= 1.5)
35. wind speed (cf= 1.5)
36. annual local glacier mass balance (snow accumulation) (cf= 1.5)
37. winter local glacier mass balance (snow accumulation) (cf= 1.5)
38. cutoff size of compartments below which compartments are added to the underlying compartment (cf= 2)
39. factor X_2 in density function (Equation S7) (cf= 1.5)
40. factor X_3 in density function (Equation S7) (cf= 1.2)
41. aerodynamic roughness length on the glacier (cf= 1.2)
42. pore close off density (cf= 1.05)
43. surface roughness wavelength (cf= 2)
44. molecular diffusivity in the atmosphere (cf= 1.05)
45. factor by how much the density of the surface compartment increases in summer (cf= 1.5)
46. factor for refreezing (fraction of dM_{ice} for additional melt on the glacier surface and refreezing) (cf= 2)
47. depth to which refreezing is active (cf= 1.5)
48. depth to which meltwater runnoff is active (cf= 1.5)
49. depth to which particle runoff is active (cf= 1.5)
50. depth to which particle relocation is active (cf= 1.5)
51. maximum fraction of particles washed out from glacier for runoff (cf= 10)
52. maximum fraction of particles washed out from glacier for relocation (cf= 10)
53. fraction of particles in the particle layer that are washed off (not used in this model version)
54. size of particle layer (not used in this model version)
55. PCB concentration in the free troposphere used for chemical input to the model
56. PCB concentration in the planetary boundary layer used for chemical input to the model

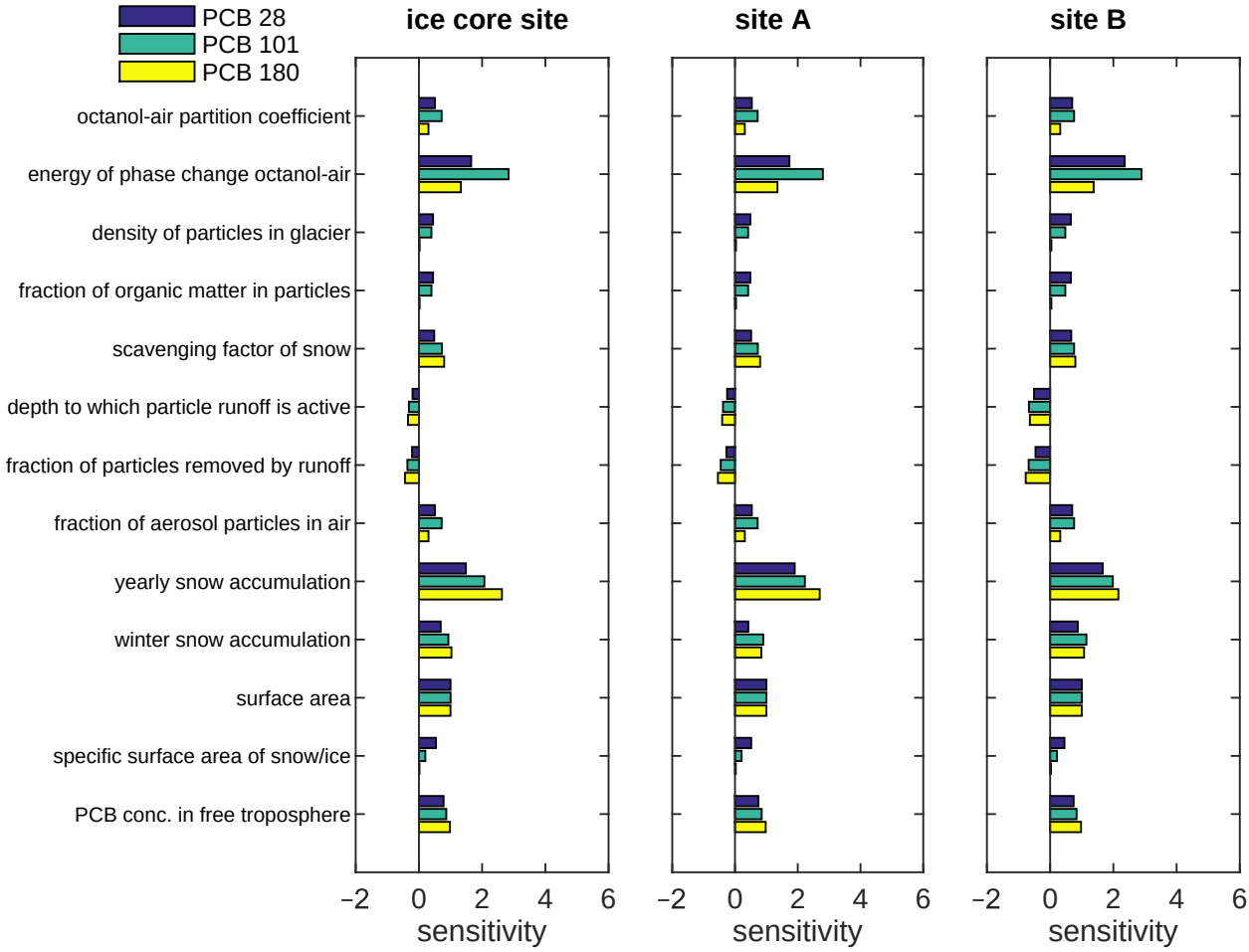

Figure S13: Results of the sensitivity analysis for PCB 28 (blue bars), 101 (green bars), and 180 (yellow bars), on the ice core site, site A, and site B. Sensitivity is calculated for the total amount of chemicals stored in the glacier in 2010. Only parameters with a sensitivity of more than 0.5, or less than -0.5 are shown.

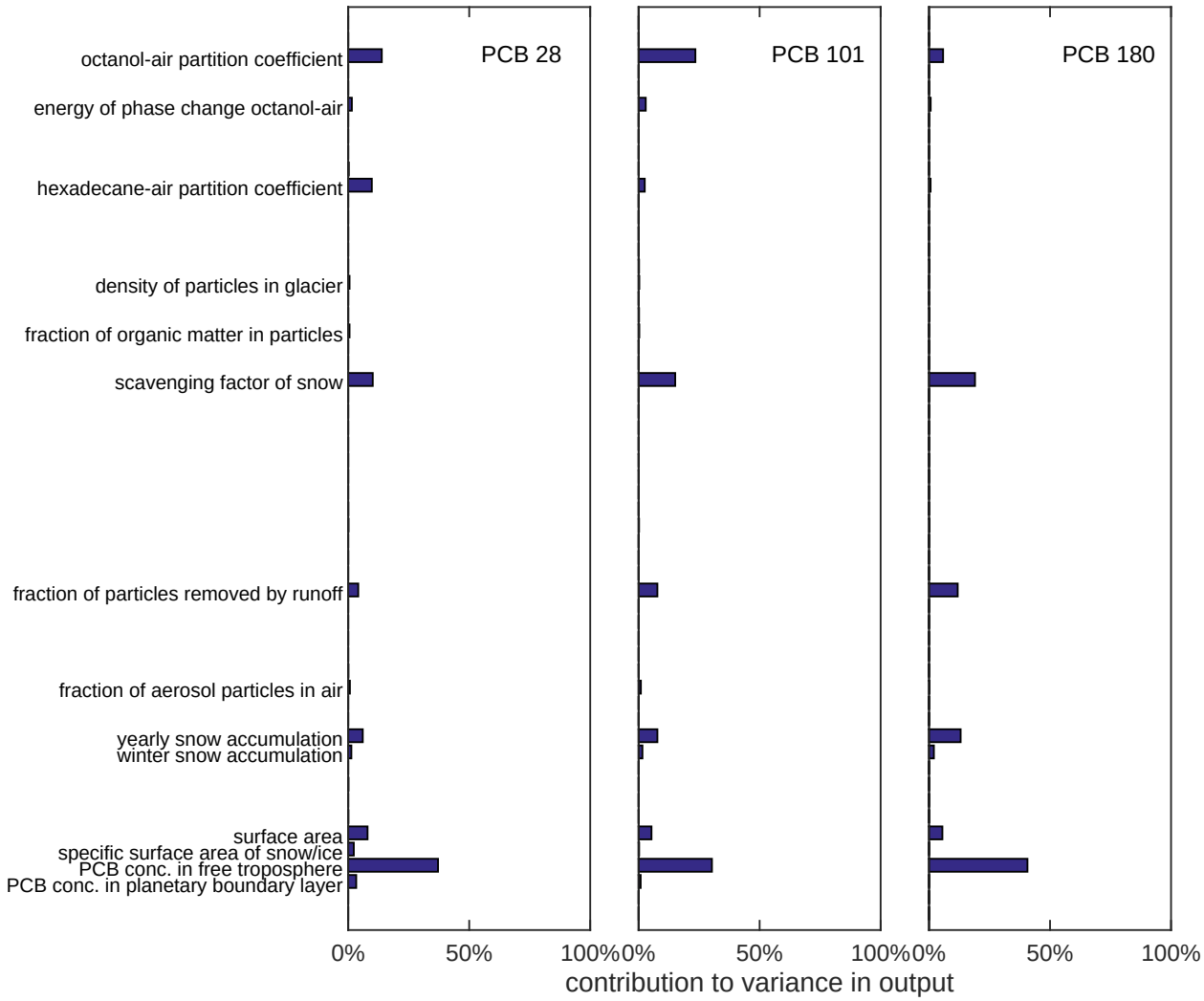

Figure S14: Parameter uncertainty analysis on the amount of chemicals stored in the glacier column in December 2010 at the ice core site. The contribution to variance of the output is shown for the 56 parameters included in the sensitivity and uncertainty analysis. Only the names of parameters having a contribution of more than 0.5% are shown in the Figure.

S9 Model Validation

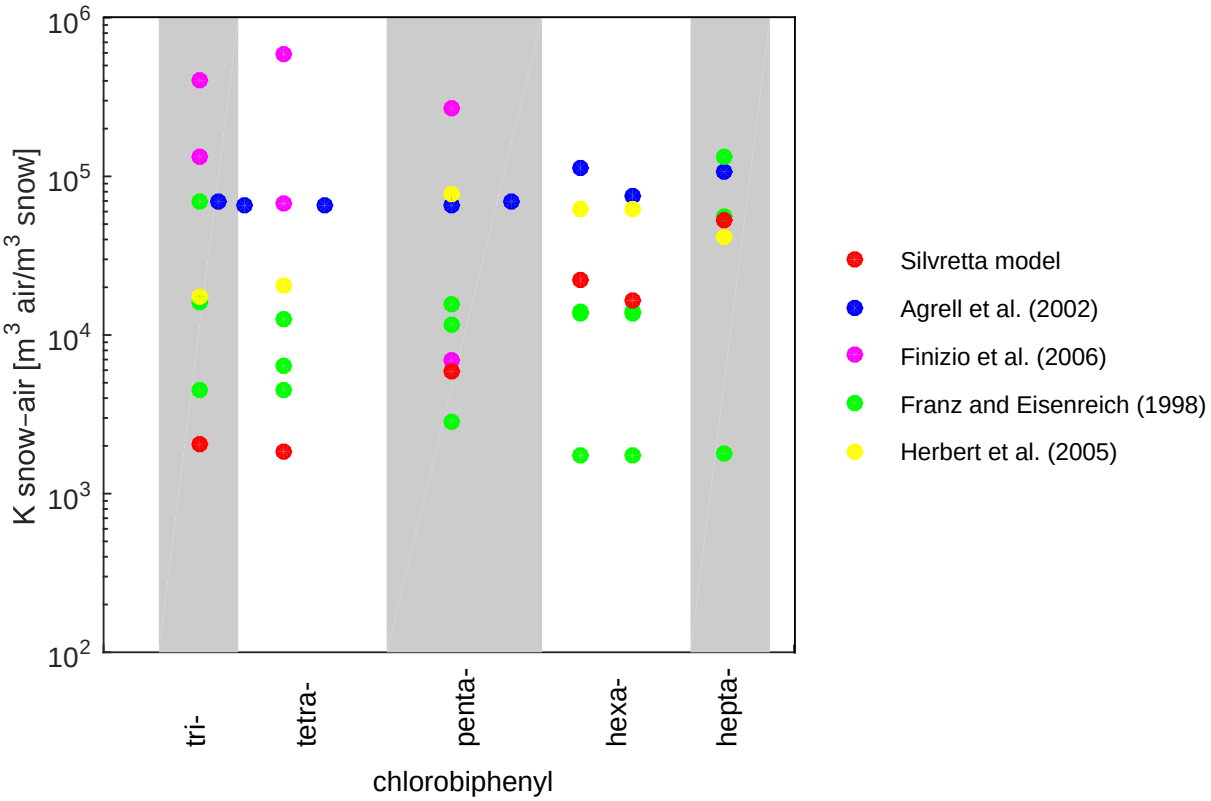

Figure S15: Snow/ice-air partition coefficients estimated using the Roth et al. method (Silvretta model, [32]), and calculated from air and snowfall concentrations [15, 3], or from air concentrations and concentrations in freshly fallen snow on the ground [20, 13] reported in the literature. All partition coefficients are corrected for a temperature of 0 °C. The values from Franz and Eisenreich [15] and Herbert et al. [20] are corrected for the particle fraction, the values from Agrell et al. [3] and Finizio et al. [13] are not particle corrected. The data is shown for tri- (PCB 28), tetra- (PCB 52), penta- (PCB 101), hexa- (PCB 138, PCB 153), and hepta- (PCB 180) chlorobiphenyl. The data of Agrell et al. is valid for individual congeners, the other studies report data for tri-, tetra-, penta-, hexa-, and heptachlorobiphenyl. The measured partition coefficients have a large variability. However, for the lower-chlorinated congeners, the Roth et al. method clearly underestimates the sorption to the ice/snow surface.

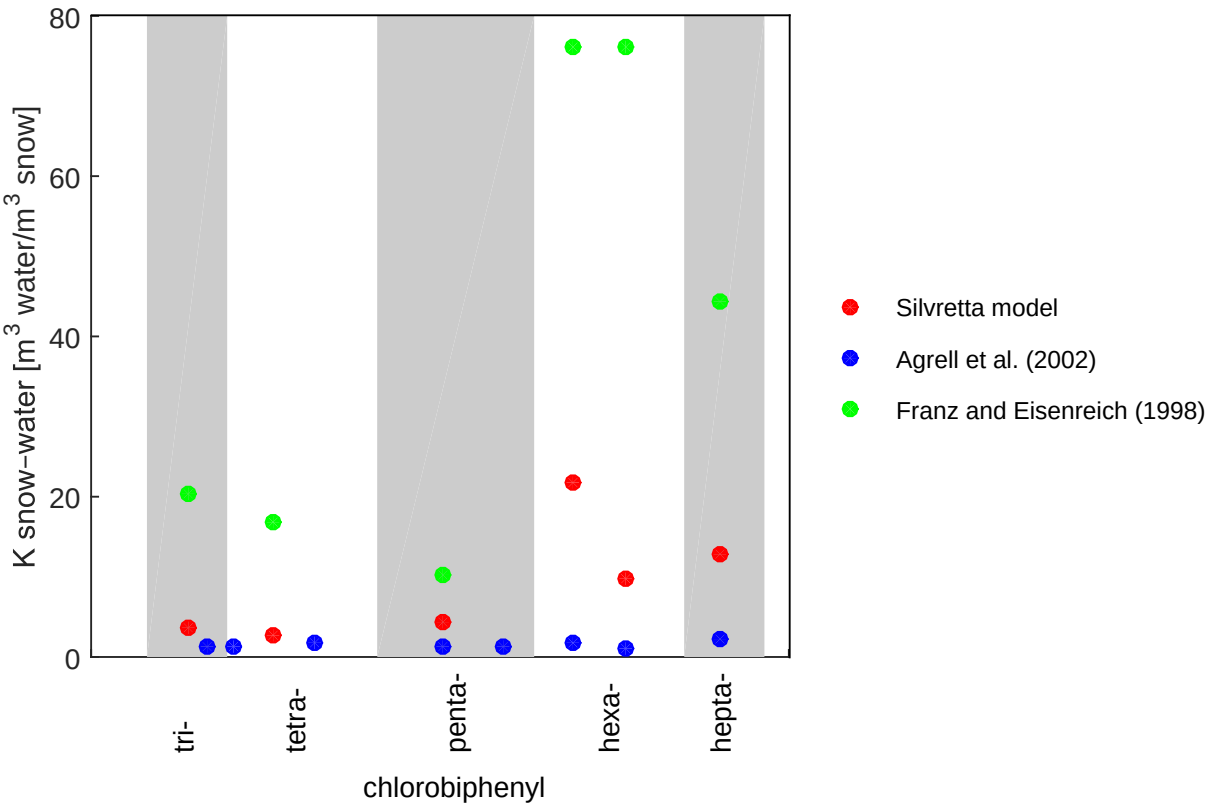

Figure S16: Modeled and measured snow/ice–water partition coefficients. In the Silvretta model, snow/ice-water partitioning is calculated using the Roth et al. method [32] and air–water partition coefficients from Schenker et al. [33] (snow–water partition coefficient = snow–air partition coefficient / water–air partition coefficient). Similarly, the literature values are calculated from measured PCB concentrations in air, rain, and snow [15, 3]. All partition coefficients are corrected for a temperature of 0 °C, and shown for tri- (PCB 28), tetra- (PCB 52), penta- (PCB 101), hexa- (PCB 138, PCB 153), and hepta- (PCB 180) chlorobiphenyl.

S10 Results

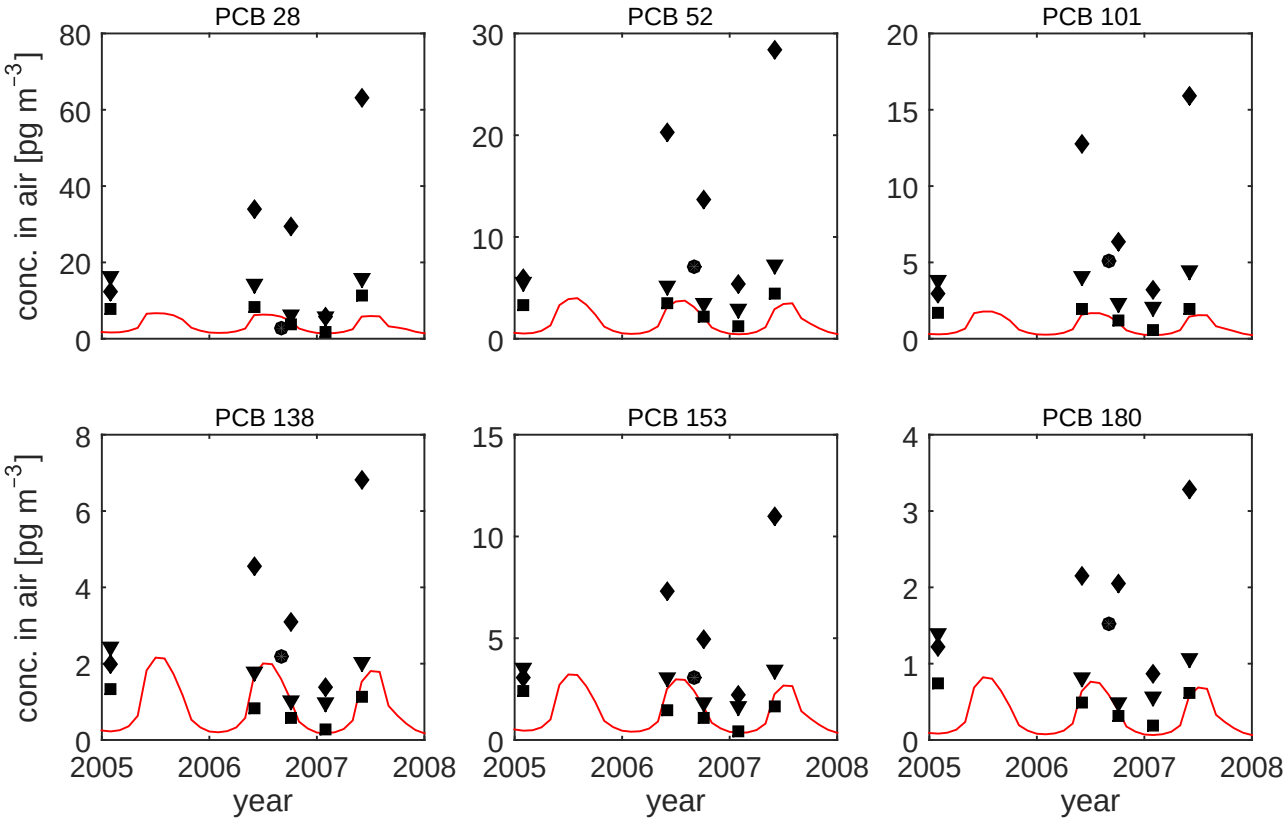

Figure S17: Modeled (red line) and measured (black markers, [29]) PCB concentrations in the atmosphere for the years 2005, 2006, and 2007. The measurements were done on Sonnblick (squares, 3100 m a.s.l., 250 km from Silvretta glacier), Weissfluhjoch (diamonds, 2660 m a.s.l., 20, km from Silvretta glacier), and Zugspitze (triangles, 2650 m a.s.l., 100 km from Silvretta glacier).

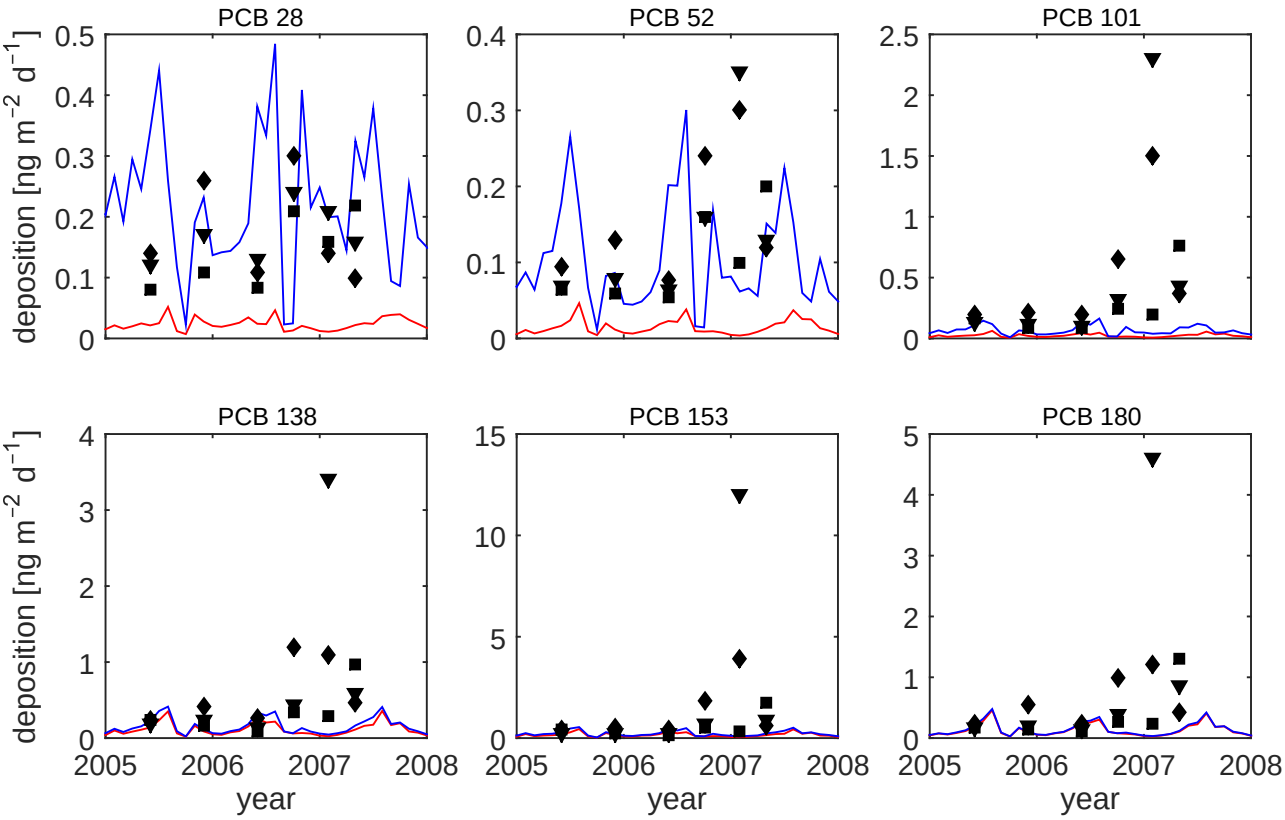

Figure S18: Modeled (red and blue lines) and measured (black markers, [29]) PCB deposition fluxes for the years 2005, 2006, and 2007. The red line corresponds to the sum of wet gaseous, wet particle, and dry particle deposition. The blue line includes the dry gaseous deposition in addition to the other three air-to-glacier transfer processes. The markers indicate measured deposition on Sonnblick (squares), Weissfluhjoch (diamonds), and Zugspitze (triangles). In contrast to the modeled transfer in Figure 3, the modeled transfer here includes deposited chemicals lost by runoff during summer rain.

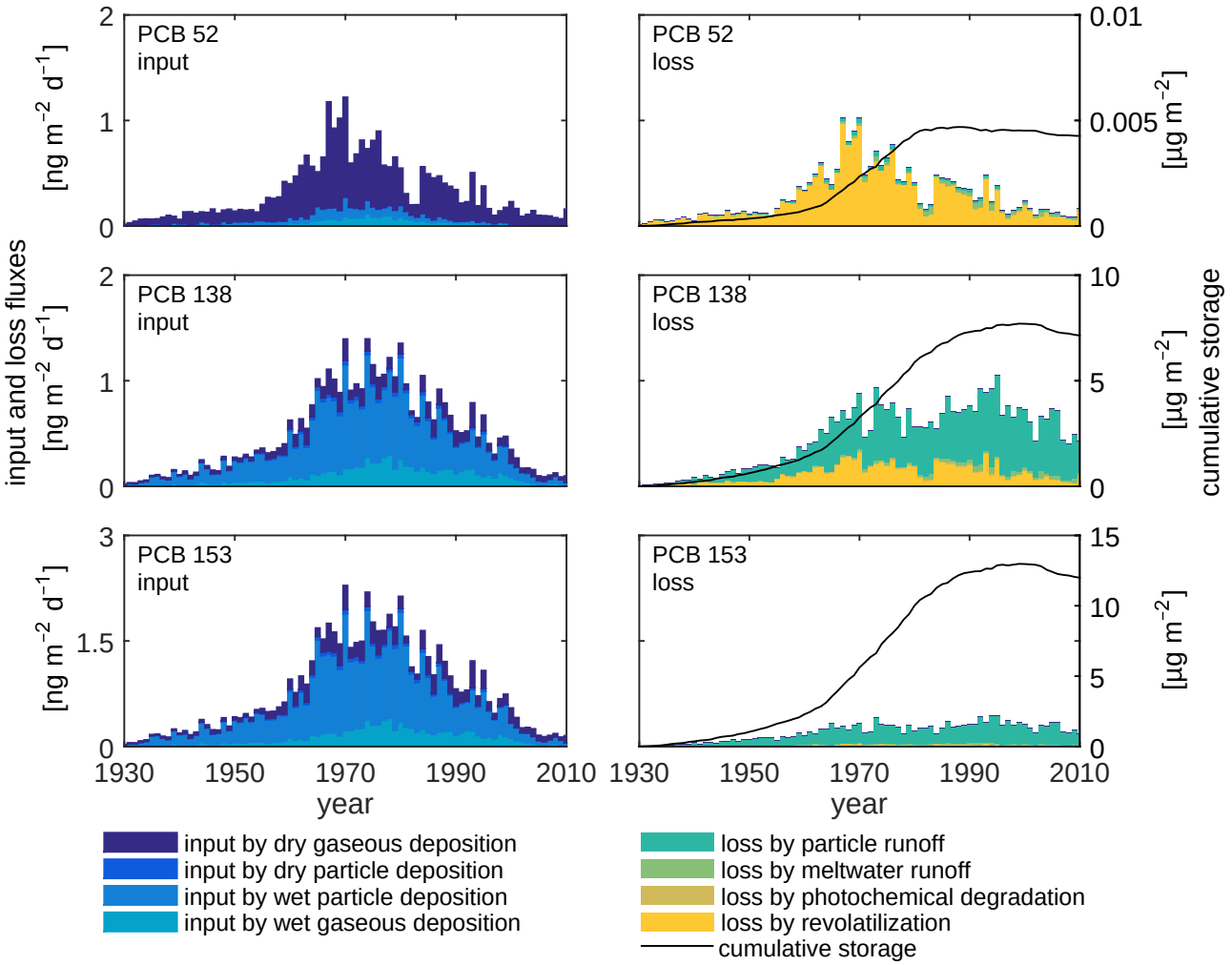

Figure S19: Fate of PCB 52, 138, and 153 at the ice core site between 1930 and 2010. Air-to-glacier transfer by dry gaseous, dry particle, wet particle, and wet gaseous deposition (left side, left axis), and loss by particle runoff, meltwater runoff, photochemical degradation, and revolatilization (right side, left axis). The black line indicates the cumulative storage in the glacier column (right side, right axis).

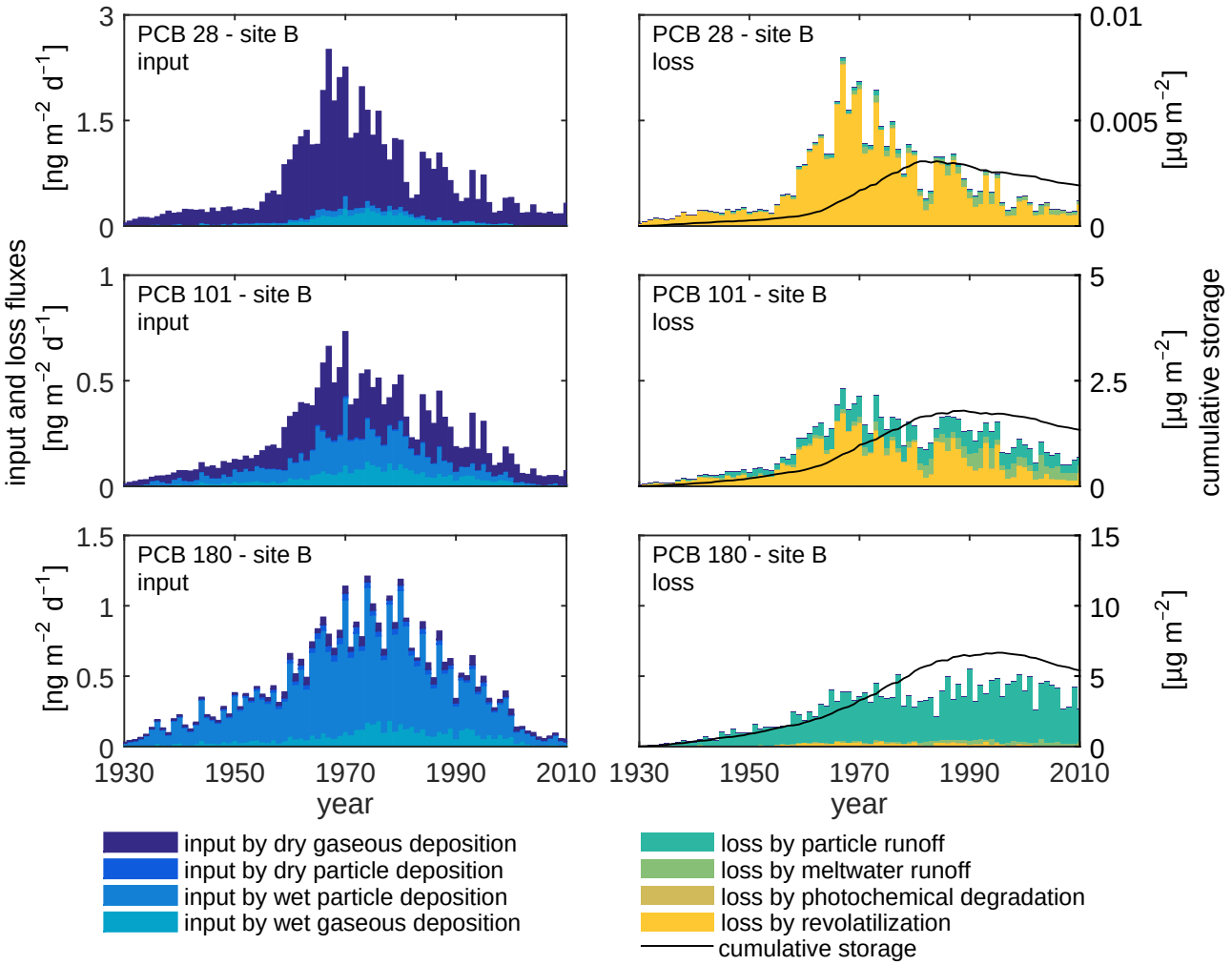

Figure S20: Fate of PCB 28, 101, and 180 at site B between 1930 and 2010. Air-to-glacier transfer by dry gaseous, dry particle, wet particle, and wet gaseous deposition (left side, left axis), and loss by particle runoff, meltwater runoff, photochemical degradation, and revolatilization (right side, left axis). The black line indicates the cumulative storage in the glacier column (right side, right axis).

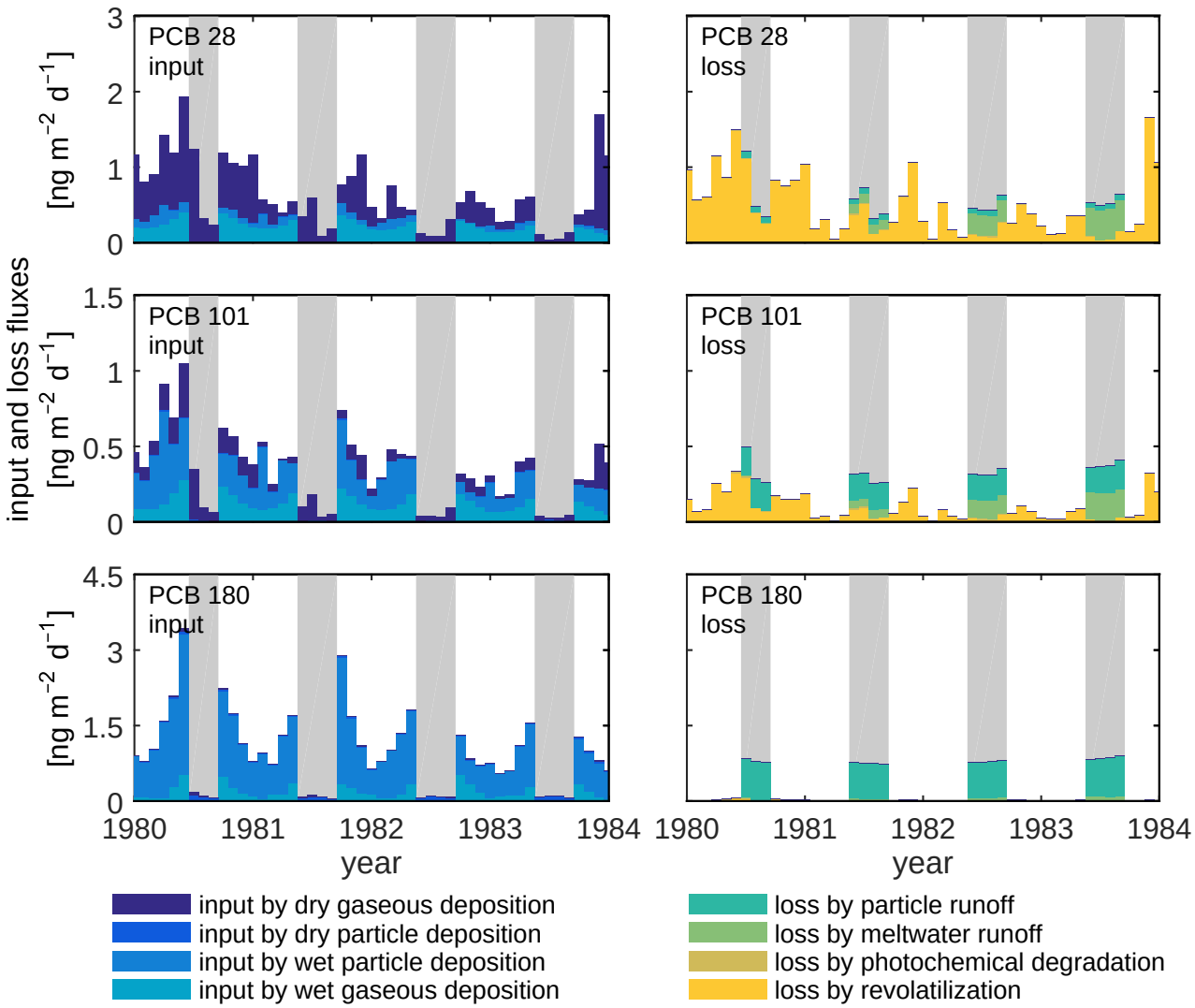

Figure S21: Seasonal fluxes of dry gaseous deposition, dry particle deposition, wet particle deposition, wet gaseous deposition, particle runoff, meltwater runoff, photochemical degradation, and revolatilization of PCB 28, 101, and 180, between 1980 and 1984. The summer months are indicated by a gray background. Dry gaseous deposition transfers chemicals from the air to the glacier surface in summer, the other deposition processes are modeled as loss processes during summer. Loss processes by particle runoff and meltwater runoff are only active in summer. The different processes active during winter and summer lead to different fate of chemicals depending on the season. The variations during the summer months depend on meteorological parameters, such as precipitation, temperature, etc.

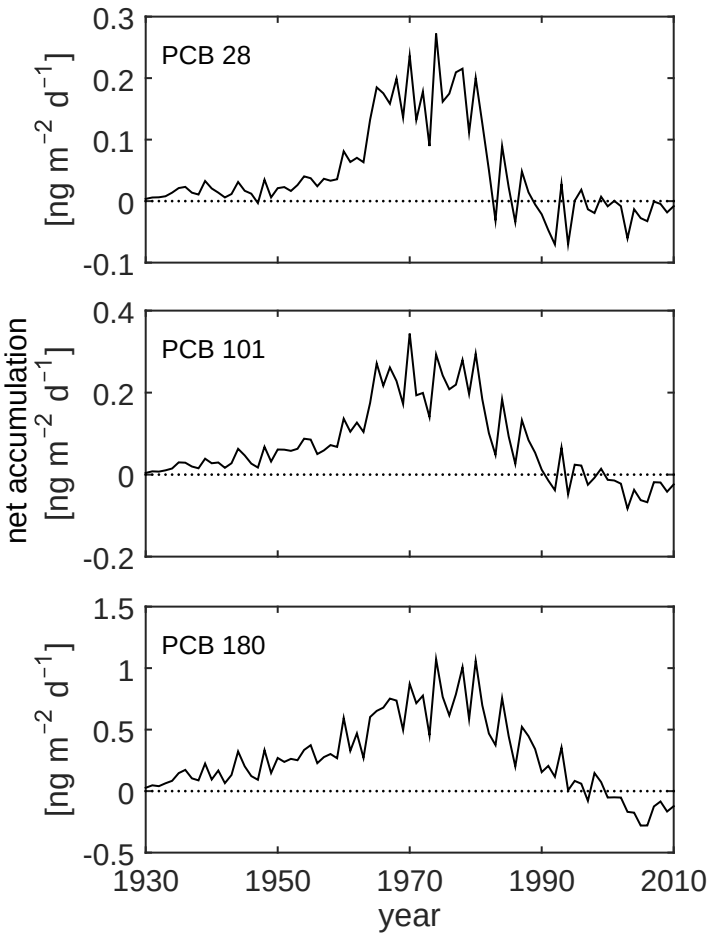

Figure S22: Net accumulation (deposition fluxes minus loss fluxes) of PCB 28, 101, and 180 between 1930 and 2010.

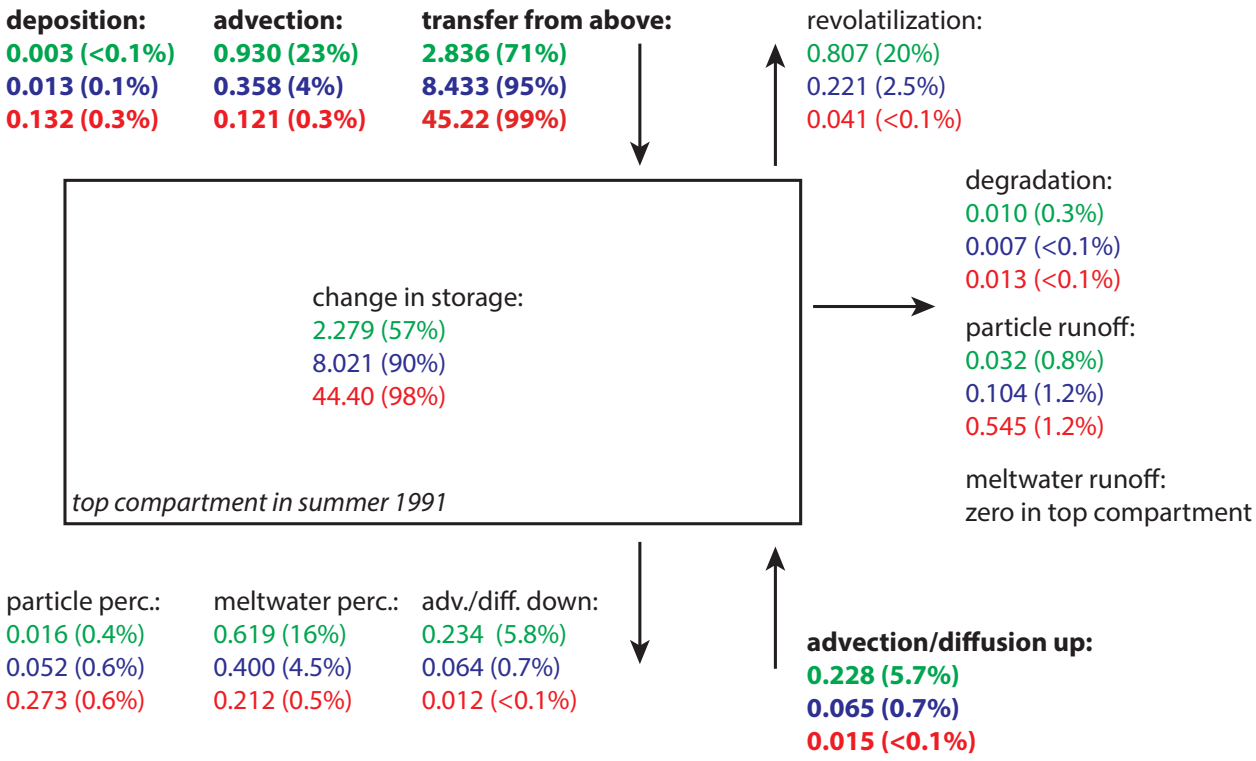

Figure S23: Input and loss fluxes to and from the surface glacier compartment during the summer 1991 (July, August, and September). The fluxes of PCB 28 (green), PCB 101 (blue), and PCB 180 (red) are in ng m^{-2} d^{-1}. Input fluxes (deposition, advection, transfer from overlying compartments that melt in the specific month, and upwards air advection/diffusion) are shown in bold font. Loss fluxes from the compartment include revolatilization, degradation, particle runoff, meltwater runoff, particle percolation, meltwater percolation, and downwards air advection/diffusion. The change in storage corresponds to the change in the amount of chemical stored in the surface glacier compartment. All values in percent correspond to 100% of the sum of all the input fluxes. The glacier mass balance during the three summer months was –0.51 m weq $month^{-1}$, indicating a strong mass loss. As a consequence, the number of compartments in the model decreases from 428 to 421 in July, from 421 to 416 in August, and from 416 to 412 in September. The fluxes shown here are valid for the surface compartment, this means compartment 421 in July, 416 in August, and 412 in September.

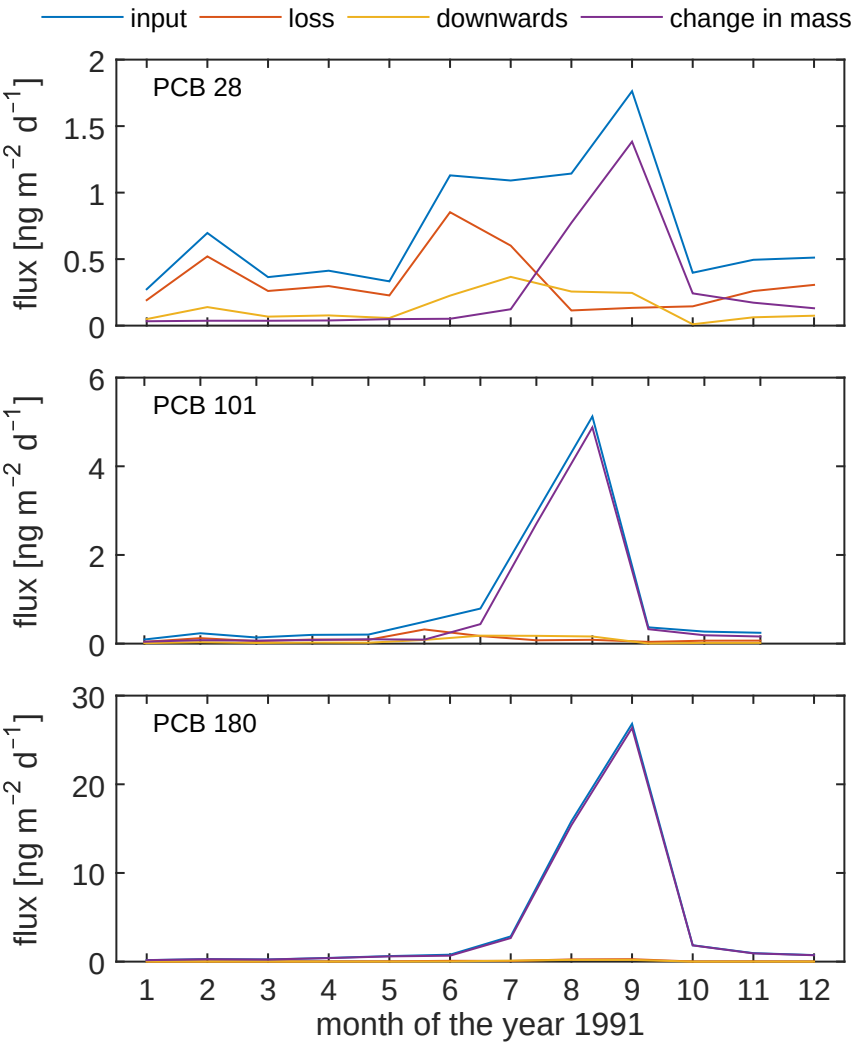

Figure S24: Input and loss fluxes to and from the surface glacier compartment in the year 1991, for PCB 28, PCB 101, and PCB 180, in ng m^{-2} d^{-1}. The input fluxes include deposition, advection, transfer from melting overlying compartments, and upwards air advection/diffusion. The loss fluxes include revolatilization, degradation, particle and meltwater runoff, particle and meltwater percolation, and downwards air advection/diffusion. The change in mass corresponds to the change in the amount of chemical stored in the surface glacier compartment. The importance of chemical enrichment at the glacier surface in summer can be seen by the high values of input and change in mass during the summer months, compared to the low values of loss and downward fluxes in the same season, especially for the higher-chlorinated congeners.

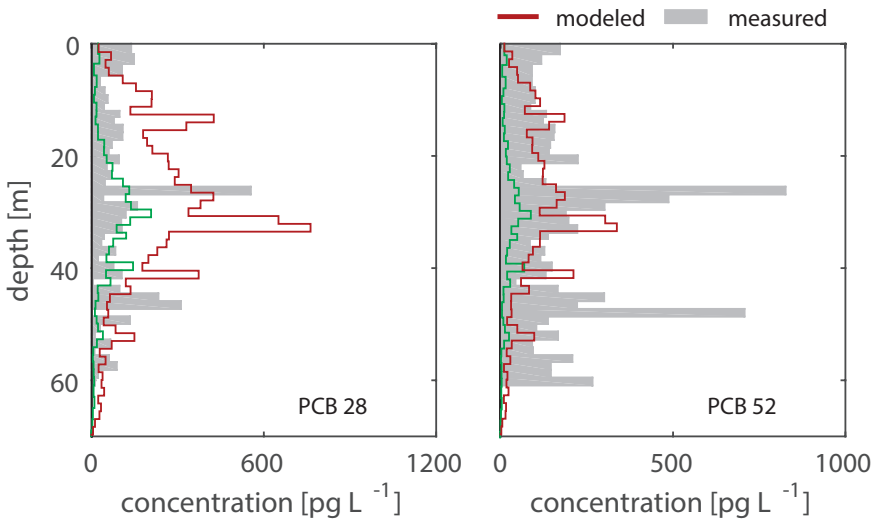

Figure S25: Concentration depth profiles of PCB 28 and PCB 52 when the snow–air partition coefficient is increased by a factor of 10 (red), compared to the original version (Figure 2 in the manuscript, green).

References

[1] M. H. Abraham and A. J. M. Al-Hussaini. Solvation parameters for the 209 PCBs: calculation of physicochemical properties. *J. Environ. Monit.*, 7(4):295–301, 2005.

[2] A. C. Adolph and M. R. Albert. Gas diffusivity and permeability through the firn column at Summit, Greenland: measurements and comparison to microstructural properties. *Cryosph.*, 8:319–328, 2014.

[3] Cecilia Agrell, Per Larsson, Lennart Okla, and Jep Agrell. PCB congeners in precipitation, wash out ratios and depositional fluxes within the Baltic Sea region, Europe. *Atmos. Environ.*, 36(2):371–383, jan 2002.

[4] P. N. Anderson and R. A. Hites. OH Radical Reactions: The Major Removal Pathway for Polychlorinated Biphenyls from the Atmosphere. *Environ. Sci. Technol.*, 30(5):1756–1763, 1996.

[5] C. Bogdal, D. Nikolic, M. P. Lüthi, U. Schenker, M. Scheringer, and K. Hungerbühler. Release of Legacy Pollutants from Melting Glaciers: Model Evidence and Conceptual Understanding. *Environ. Sci. Technol.*, 44(11):4063–4069, 2010.

[6] T. C. Bond, E. Bhardwaj, R. Dong, R. Jogani, S. Jung, C. Roden, D. G. Streets, and N. M. Trautmann. Historical emissions of black and organic carbon aerosol from energy-related combustion, 1850–2000. *Glob. Biogeochem. Cycles*, 21(2):GB2018, 2007.

[7] K. Breivik, A. Sweetman, J. M. Pacyna, and K. C. Jones. Towards a global historical emission inventory for selected PCB congeners – A mass balance approach: 3. An update. *Sci. Total Environ.*, 377(2-3):296–307, may 2007.

[8] K. M. Cuffey and W. S. B. Paterson. *The Physics of Glaciers*. Elsevier Inc.: Burlington, MA, fourth edition, 2010.

[9] G. L. Daly and F. Wania. Simulating the Influence of Snow on the Fate of Organic Compounds. *Environ. Sci. Technol.*, 38(15):4176–4186, 2004.

[10] F. Dominé, A.-S. Taillandier, and W. R. Simpson. A parameterization of the specific surface area of seasonal snow for field use and for models of snowpack evolution. *J. Geophys. Res.*, 112(F2):F02031, jun 2007.

[11] EMEP. European Monitoring and Evaluation Programme (EMEP). Convention on Long-range Transboundary Air Pollution (CLRTAP) (accessed in October 2014). www.emep.int.

[12] Federal Commission for Air Hygiene (FCAH). Feinstaub in der Schweiz. Statusbericht der Eidgenössischen Komission für Lufthygiene (EKL). Technical report, Federal Commission for Air Hygiene (FCAH), Berne, Switzerland, 2007.

[13] A. Finizio, S. Villa, F. Raffaele, and M. Vighi. Variation of POP concentrations in fresh-fallen snow and air on an Alpine glacier (Monte Rosa). *Ecotoxicol. Environ. Saf.*, 63:25–32, 2006.

[14] A. G. Fountain and J. S. Walder. Water flow through temperate glaciers. *Rev. Geophys.*, 36(3):299–328, 1998.

[15] T. P. Franz and S. J. Eisenreich. Snow Scavenging of Polychlorinated Biphenyls and Polycyclic Aromatic Hydrocarbons in Minnesota. *Environ. Sci. Technol.*, 32(12):1771–1778, 1998.

[16] M. Gerbaux, C. Genthon, P. Etchevers, C. Vincent, and J. P. Dedieu. Surface mass balance of glaciers in the French Alps: distributed modeling and sensitivity to climate change. *J. Glaciol.*, 51(175):561–572, 2005.

[17] K.-U. Goss and R. P. Schwarzenbach. Empirical Prediction of Heats of Vaporization and Heats of Adsorption of Organic Compounds. *Environ. Sci. Technol.*, 33(19):3390–3393, 1999.

[18] A. M. Grannas, A. E. Jones, J. Dibb, M. Ammann, C. Anastasio, H. J. Beine, M. Bergin, J. Bottenheim, C. S. Boxe, G. Carber, G. Chem, J. H. Crawford, F. Domine, M. M. Frey, M. I. Guzman, D. E. Heard, D. Helmig, M. R. Hoffmann, R. E. Honrath, L. G. Huey, M. A. Hutterli, H. W. Jacobi, P. Klan, B. Lefer, J. McConnell, J. Plane, R. Sander, J. Savarino, P. B. Shepson, W. R. Simpson, J. R. Sodeau, R. von Glasow, R. Weller, E. W. Wolff, and T. Zhu. An overview of snow photochemistry: evidence, mechanisms and impacts. *Atmos. Chem. Phys. Discuss.*, 7:4165–4283, 2007.

[19] T. Harner and T. F. Bidleman. Octanol-Air Partition Coefficient for Describing Particle/Gas Partitioning of Aromatic Compounds in Urban Air. *Environ. Sci. Technol.*, 32(10):1494–1502, 1998.

[20] B. M. J. Herbert, C. J. Halsall, S. Villa, K. C. Jones, and R. Kallenborn. Rapid Changes in PCB and OC Pesticide Concentrations in Arctic Snow. *Environ. Sci. Technol.*, 39(9):2998–3005, 2005.

[21] M. Huss and A. Bauder. 20th-century climate change inferred from four long-term point observations of seasonal mass balance. *Ann. Glaciol.*, 50:207–214, 2009.

[22] M. Huss, A. Bauder, M. Funk, and R. Hock. Determination of the seasonal mass balance of four Alpine glaciers since 1865. *J. Geophys. Res.*, 113(F1):F01015, mar 2008.

[23] L. Legagneux, A. Cabanes, and F. Dominé. Measurement of the specific surface area of 176 snow samples using methane adsorption at 77 K. *J. Geophys. Res.*, 107(D17):4335–4349, sep 2002.

[24] D. Mackay. *Multimedia Environmental Models: The Fugacity Approach*. Lewis Publishers, 2001.

[25] N. Matykiewiczová, J. Klánová, and P. Klán. Photochemical Degradation of PCBs in Snow. *Environ. Sci. Technol.*, 41:8308–8314, 2007.

[26] T. Meyer and F. Wania. *Handbook of Chemical Mass Transport in the Environment: Chapter 18: Chemical Exchange between Snow and the Atmosphere*. CRC Press, oct 2010.

[27] R. J. Millington. Gas Diffusion in Porous Media. *Science (80-.).*, 130(3367):100–102, 1959.

[28] National Air Pollution Monitoring Network (NABEL). Long-term measurement series of air pollutants (accessed in October 2014). www.empa.ch/nabel.

[29] I. Offenthaler, R. Bassan, C. Belis, I. Garo-Stach, S. Ganz, S. Iozza, G. Jakobi, A. Kaiser, M. Kirchner, W. Knoth, N. Kräuchi, W. Levy, W. Moche, J. Nurmi-Legat, S. Raccanelli, K.-W. Schramm, P. Schröder, I. Sedivy, P. Simoncic, M. Staudinger, G. Thanner, M. Uhl, U. Vilhar, and P. Weiss. Monarpop: Technical Report. Federal Ministry of Agriculture, Forestry, Environment and Water Management. Vienna, Austria, 2009.

[30] P. A. Pavlova. *Accelerated release of persistent organic pollutants from alpine glaciers*. PhD thesis, University of Berne, Berne, Switzerland, 2014.

[31] P. A. Pavlova, T. M. Jenk, P. Schmid, C. Bogdal, C. Steinlin, and M. Schwikowski. Polychlorinated Biphenyls in a Temperate Alpine Glacier: 1. Effect of Percolating Meltwater on their Distribution in Glacier Ice. *Environ. Sci. Technol.*, in press, 2015.

[32] C. M. Roth, K.-U. Goss, and R. P. Schwarzenbach. Sorption of Diverse Organic Vapors to Snow. *Environ. Sci. Technol.*, 38(15):4078–4084, 2004.

[33] U. Schenker, M. MacLeod, M. Scheringer, and K. Hungerbühler. Improving Data Quality for Environmental Fate Models: A Least-Squares Adjustment Procedure for Harmonizing Physicochemical Properties of Organic Compounds. *Environ. Sci. Technol.*, 39(21):8434–8441, 2005.

[34] J. Schwander. Environmental Records in Glaciers and Ice Sheets. In *Phys. Chem. Earth Sci. Res. Reports*, pages 53–67, Berlin, 1989. Springer-Verlag Berlin.

[35] R. P. Schwarzenbach, P. M. Gschwend, and D. M. Imboden. *Environmental Organic Chemistry*. Wiley-Interscience, second edition, 2003.

[36] J. H. Seinfeld and S. N. Pandis. *Atmospheric Chemistry and Phyics: From Air Pollution to Climate Change*. Wiley, New York, 1998.

[37] C. M. Spivakovsky, J. A. Logan, S. A. Montzka, Y. J. Balkanski, M. Foreman-Fowler, D. B. A. Jones, L. W. Horowitz, A. C. Fusco, C. A. M. Brenninkmeijer, M. J. Prather, S. C. Wofsy, and M. B. McElroy. Three-dimensional climatological distribution of tropospheric OH: Update and evaluation. *J. Geophys. Res. Atmos.*, 105(D7):8931–8980, 2000.

[38] C. Steinlin, C. Bogdal, M. Scheringer, P. A. Pavlova, M. Schwikowski, P. Schmid, and K. Hungerbühler. Polychlorinated Biphenyls in Glaciers. 2. Model Results of Deposition and Incorporation Processes. *Environ. Sci. Technol.*, 48(14):7849–7857, 2014.

[39] Swiss Federal Office of Meteorology and Climatology (MeteoSwiss). Climate norm values 1961–1990 and 1981–2010 (accessed in October 2014).

[40] Swiss Federal Office of Meteorology and Climatology (MeteoSwiss). IDAweb. The data portal of MeteoSwiss for research and teaching (accessed in October 2014). www.meteoswiss.ch.

[41] P. C. M. van Noort, J. J. H. Haftka, and J. R. Parsons. Updated Abraham Solvation Parameters for Polychlorinated Biphenyls. *Environ. Sci. Technol.*, 44(18):7037–7042, 2010.

[42] Laboratory of Hydraulics Hydrology (VAW) and Glaciology. Swiss Glaciers Monitoring Network (accessed in October 2014). http://glaciology.ethz.ch/messnetz.

[43] J. M. Wallace and P. V. Hobbs. *Atmospheric Science: An Introductory Survey*. Elsevier, 2006.

[44] H. Wöhrnschimmel, M. Macleod, and K. Hungerbühler. Emissions, fate and transport of persistent organic pollutants to the Arctic in a changing global climate. *Environ. Sci. Technol.*, 47(5):2323, 2013.